QUARTERLY IMAGE QUALITY REPORT

IQR#022

Reporting period from 16/03/2019 to 15/06/2019

Reference: *PROBA-V_D9_QIR-022_2019-Q2_v1.0*
Author(s): Sindy Sterckx, Stefan Adriaensen, Iskander Benhadj, Erwin Wolters
Version: 1.0
Date: 20/03/2019

DOCUMENT CONTROL

Signatures

Author(s) Sindy Sterckx, Stefan Adriaensen, Erwin Wolters, Iskander Benhadj

Reviewer(s) Dennis Clarijs

Approver(s) Dennis Clarijs

Issuing authority VITO N.V.

Change record

Release	Date	Pages	Description	Editor(s)/Reviewer(s)
1.0	20/06/2019	All	Initial version	

TABLE OF CONTENT

1. Radiometric Image Quality

1.1. Summary

Before updating the ICP files on the basis of the yaw-based equalization corrections, an assessment is made on the impact of the corrections on actual images taken over relatively uniform desert sites. Visual analyses (see chapter 1.4) indicate a clear improvement of the non-uniformities in the scene, both for low and high frequency variations. The operational ICP files will now be updated to include the yaw-based corrections of the equalization coefficients.

The DCC calibration results (see 1.2.2.1) show a decrease in responsivity of the BLUE bands of all cameras, even after May 2017 when the degradation model for BLUE LEFT/CENTER strips was implemented (see 1.2.3.1). Please note that for BLUE RIGHT strip no degradation model is applied as no degradation is observed on the basis of the OSCAR Libya-4 results (see 1.2.1.1). A possible explanation for the trend observed in the DCC BLUE band results, is the increase of responsivity in the RED band as observed in the Libya-4 results for all cameras as well as in the moon calibration results for the CENTER camera.
As the BLUE band DCC results, are inter-band calibration results, expressed relatively to the RED band, an increase in responsivity of the RED band (and not for the BLUE band) will result in a decrease of the BLUE band DCC inter-band calibration results.

During Q2 of 2019 three new bad pixels were identified: Left SWIR1 PixelID 717, Left SWIR3 PixelID82 and Center SWIR1 PixelID448.

.

1.2. Assessment of the radiometric accuracy

1.2.1. Absolute radiometric accuracy

The absolute radiometric calibration requirement for PROBA-V specifies a 5 % absolute accuracy. This requirement is assessed through vicarious calibration over Libya-4 desert site and Rayleigh calibration zones.

1.2.1.1. Libya-4 desert calibration

Methodology

The nominal approach for assessing the absolute radiometric accuracy relies on the comparison between cloud-free TOA reflectance as measured over the Libya-4 desert site by PROBA-V and the modelled TOA reflectance values, following the approach described in [LIT1]. Validation of the approach using various satellite data (i.e. AQUA-MODIS, MERIS, AATSR, PARASOL, SPOT-VGT) has shown that absolute calibration over the Libya-4 desert is achievable with this approach with an accuracy of 3% [LIT1, LIT2].

Results

In Figure1, Figure3 and Figure 5 the monthly averaged results ($avg(\rho_{TOA}^{k,ProbaV(Acom)}/\rho_{TOA}^{k,model})$) and its standard deviation are given for respectively LEFT, CENTER and RIGHT camera.
The individual area-averaged results are given in Figure2, Figure4 and Figure 6 with a 3 % error bar (as expected uncertainty for an individual result) for respectively VNIR and SWIR strips.

Results are obtained based on the **Collection 1** ICP files.

Since October 2018 a degradation model (see section 1.2.3) is no longer applied to the SWIR absolute calibration coefficients as the current linear model resulted in an overcorrection of the degradation in the SWIR.

An increase in responsivity of the RED band of the different cameras is observed over the whole mission. Currently this increase of responsivity is not yet corrected for the ICP files (i.e. calibration coefficients of RED band not changed since start operational phase).

Since May 2017 the LEFT and CENTER absolute calibration coefficients for the BLUE band are monthly updated following a linear degradation model (see section 1.2.3). The slight degradation observed in the BLUE band desert results for LEFT and CENTER camera are probably due to degradation in the first years for which a degradation model was not yet in place.
As no decrease in responsivity is observed in the Libya-4 results for the BLUE band of the RIGHT camera, a degradation model is not yet in place for this camera/band.

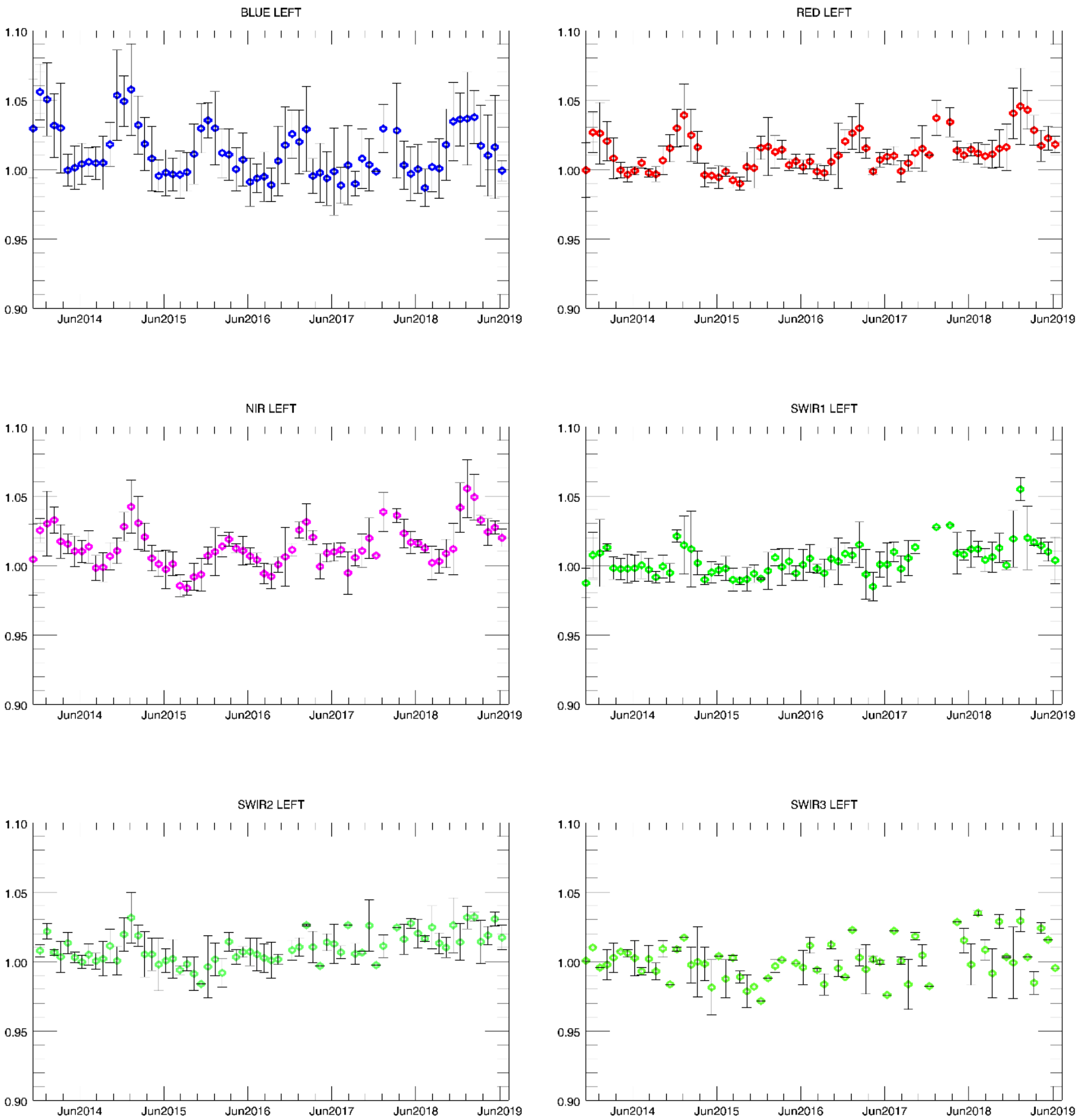

Figure 1. Libya-4 desert calibration results: LEFT monthly averaged results (Collection 1)

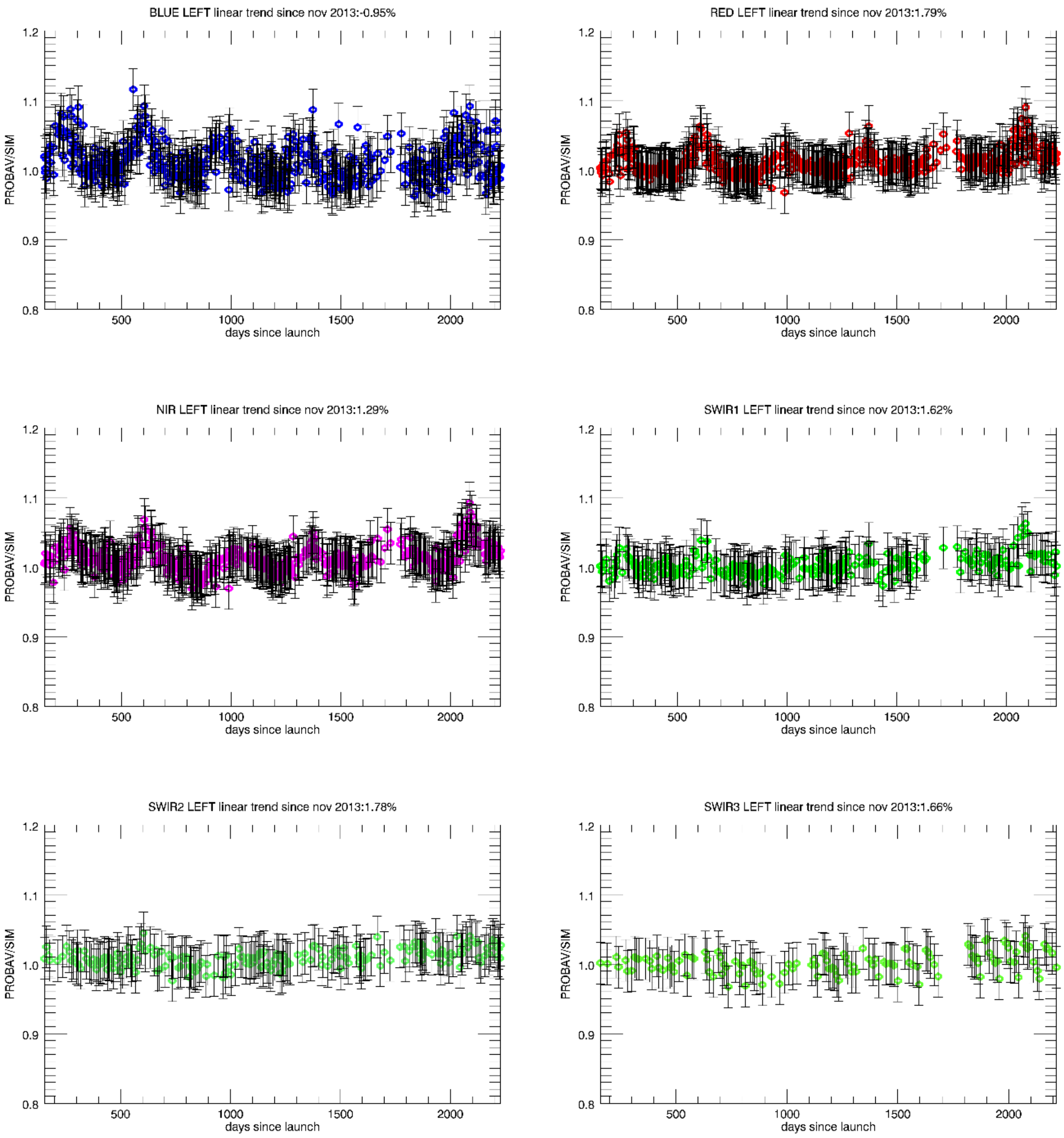

Figure 2. Libya-4 desert calibration results: LEFT individual results (Collection 1)

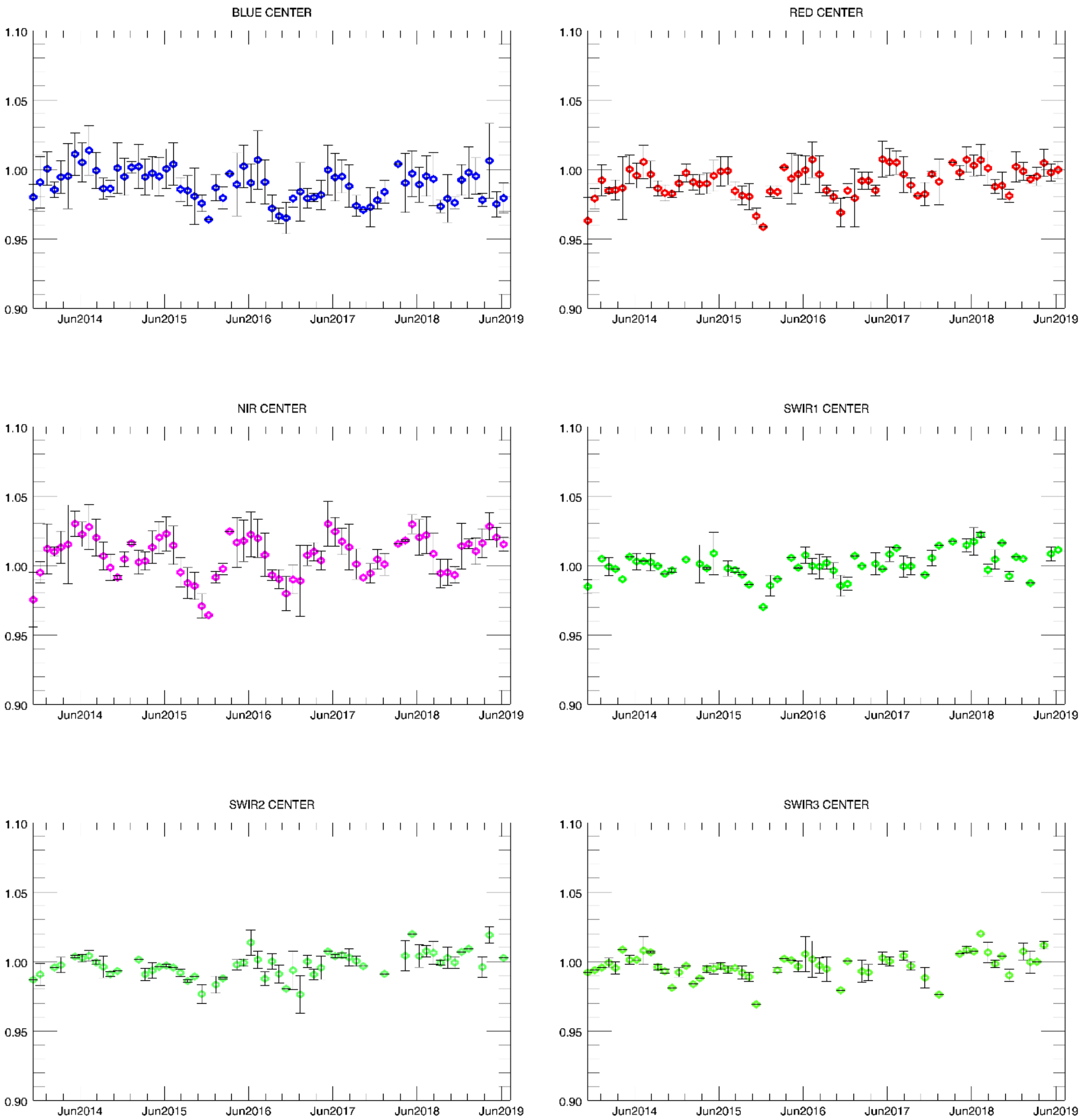

Figure 3. Libya-4 desert calibration results: CENTER monthly averaged results (Collection 1)

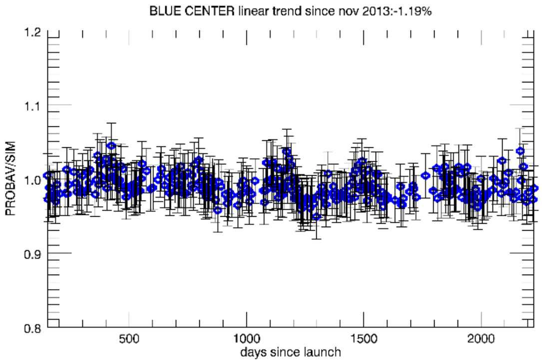
BLUE CENTER linear trend since nov 2013:-1.19%
PROBAV/SIM
days since launch

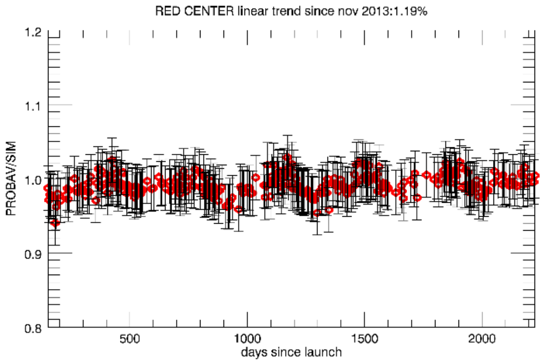
RED CENTER linear trend since nov 2013:1.19%
PROBAV/SIM
days since launch

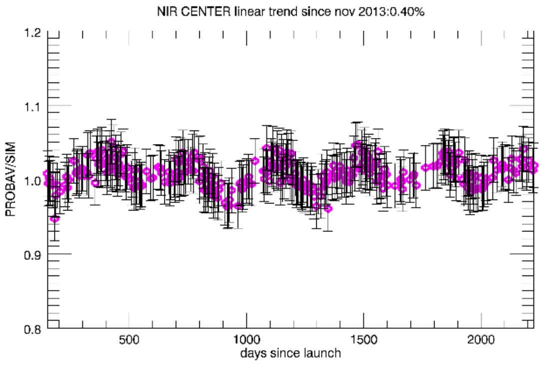
NIR CENTER linear trend since nov 2013:0.40%
PROBAV/SIM
days since launch

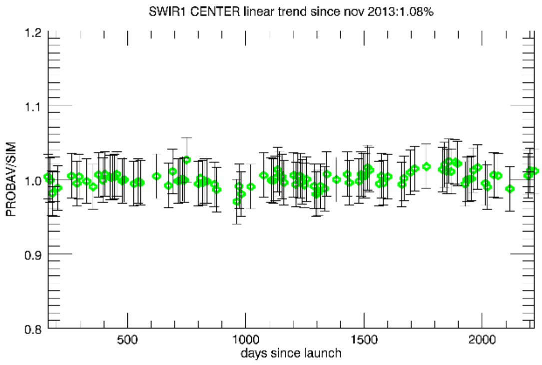
SWIR1 CENTER linear trend since nov 2013:1.08%
PROBAV/SIM
days since launch

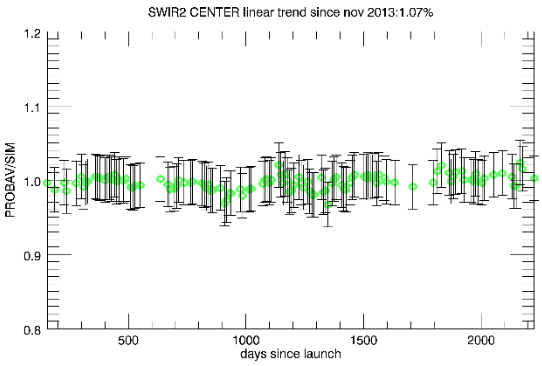
SWIR2 CENTER linear trend since nov 2013:1.07%
PROBAV/SIM
days since launch

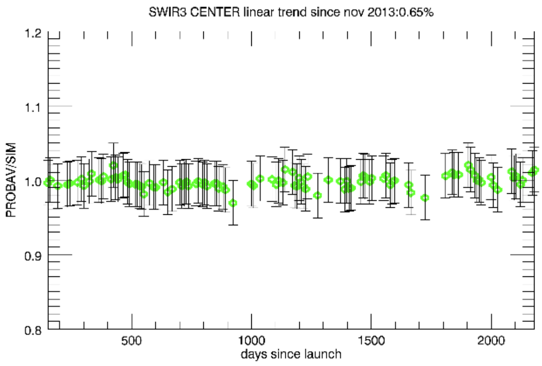
SWIR3 CENTER linear trend since nov 2013:0.65%
PROBAV/SIM
days since launch

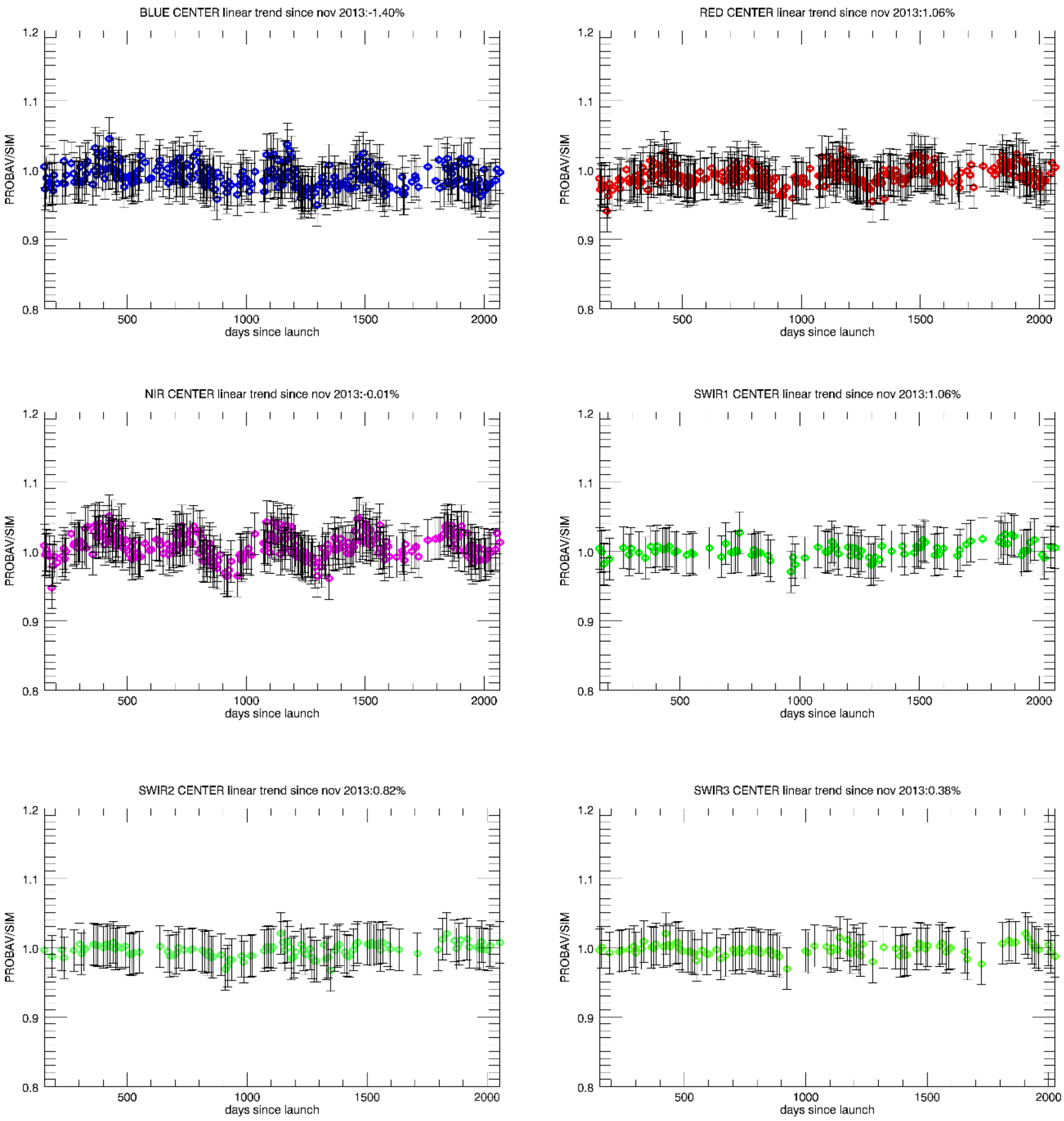

Figure 4. Libya-4 desert calibration results: CENTER individual results (Collection 1)

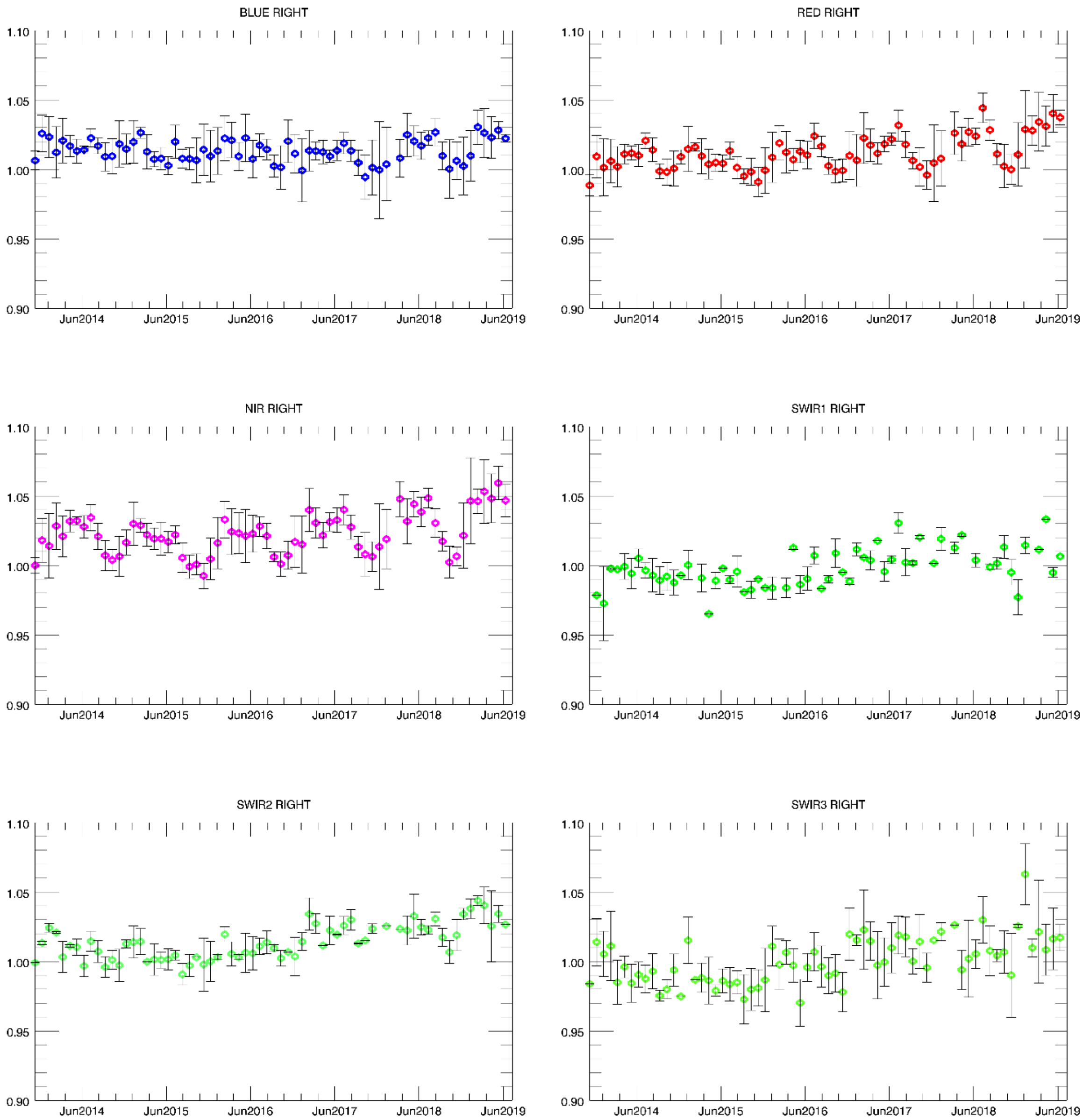

Figure 5. Libya-4 desert calibration results: RIGHT monthly averaged results (Collection 1)

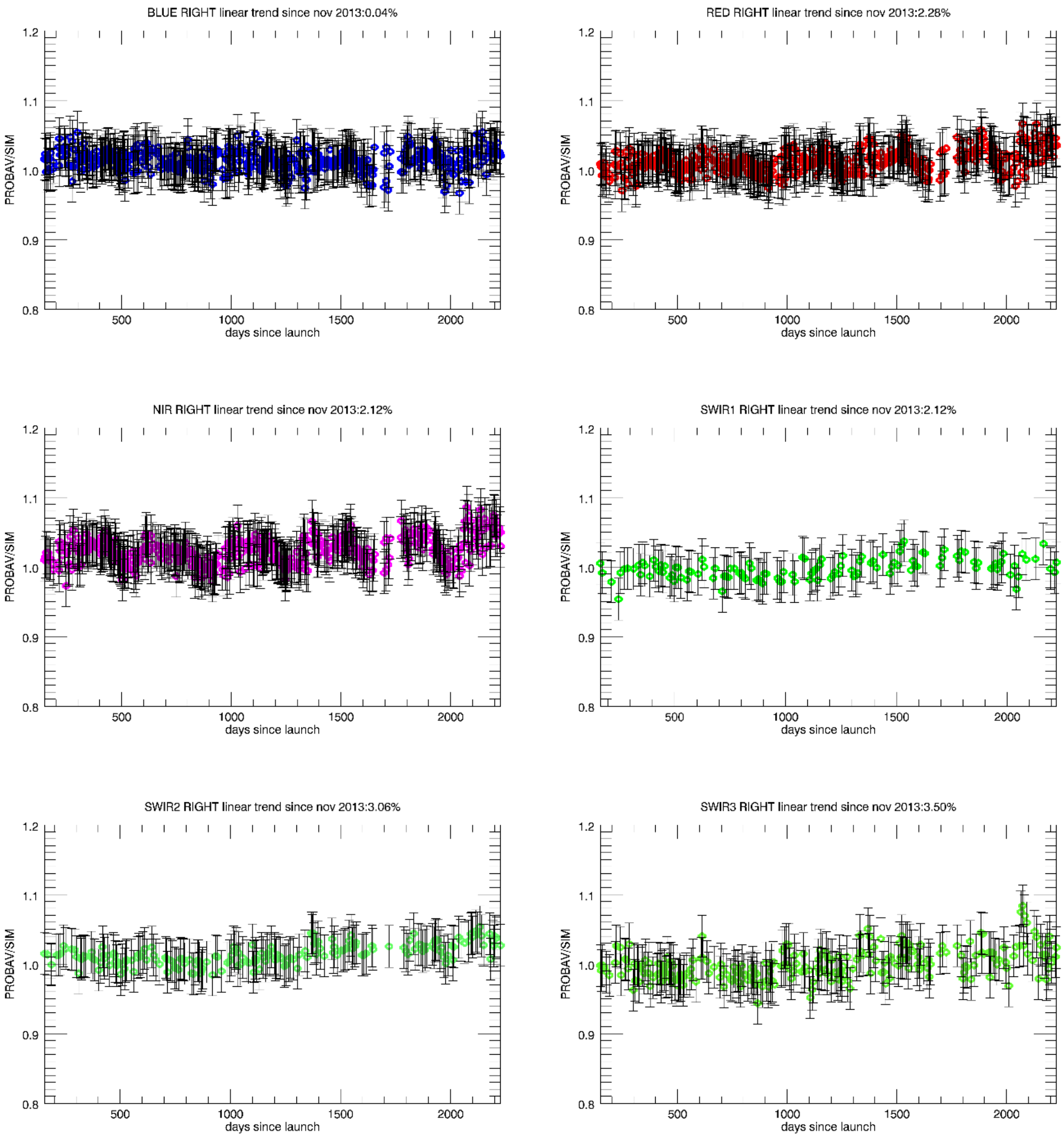

Figure 6. Libya-4 desert calibration results: RIGHT individual results (Collection 1)

1.2.1.2. Rayleigh calibration

Methodology

The Rayleigh calibration approach is an absolute calibration method for BLUE and RED bands. The primary assumption of the approach is that the ocean does not contribute to the Top-Of-Atmosphere (TOA) signal in the NIR. The contribution of aerosol scattering is derived from the ***NIR reference band*** where molecular scattering is negligible. The aerosol content estimated from the NIR band is then transferred to the BLUE and RED band to model the TOA radiance with a radiative transfer code. The simulated radiance values are then compared with the measured values.

Results

The scene averaged Rayleigh results (($\rho_{TOA}^{k,ProbaV(Acom)}/\rho_{TOA}^{k,model}$)) (with a 4 % error bar as rough indication of uncertainty of one individual result) obtained since January 2014 for LEFT, CENTER and RIGHT camera are given in respectively Figure 7, Figure 8 and Figure 9.

Results are obtained using the **Collection 1 ICP** files.

No significant trend is visible in the Rayleigh calibration results.

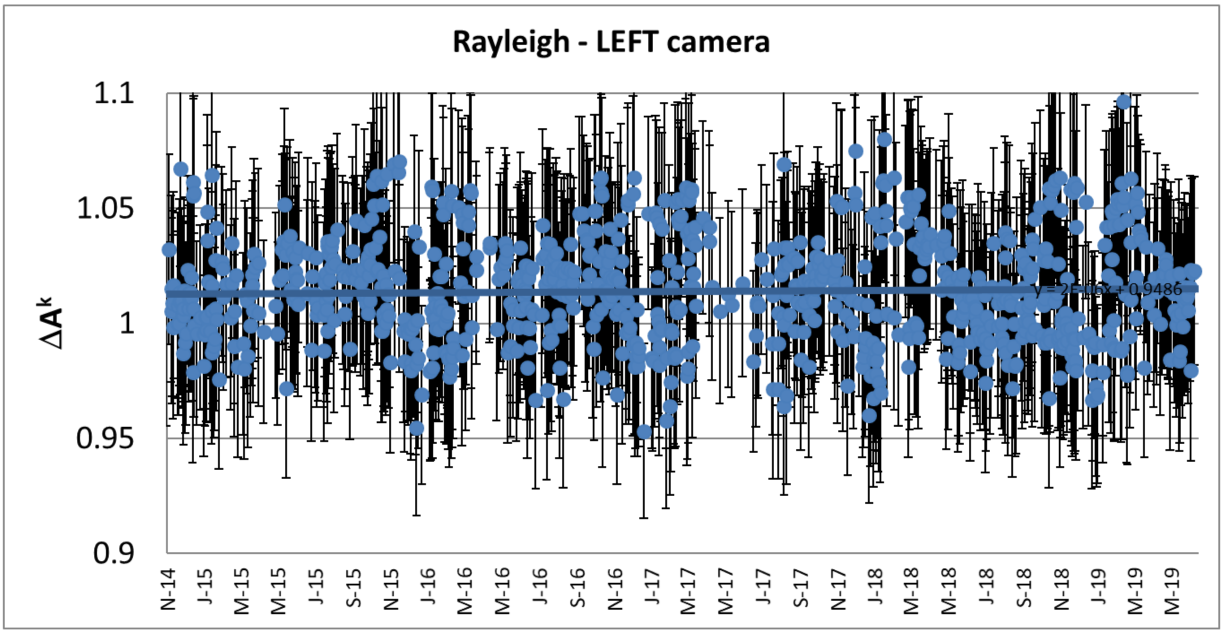

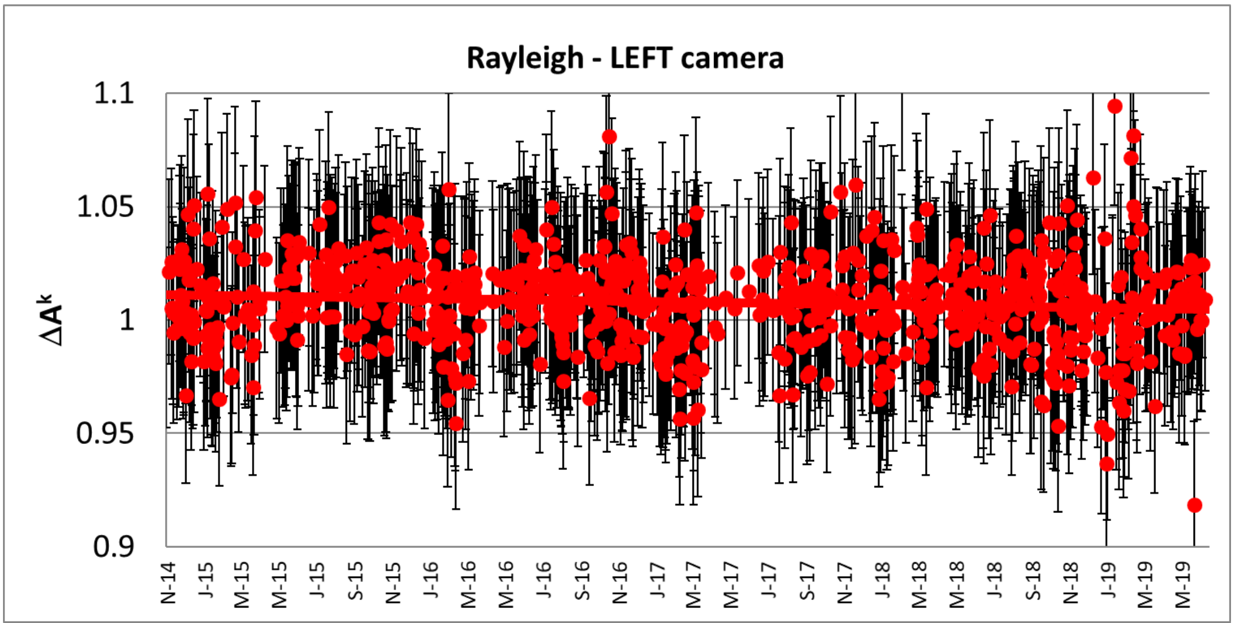

Figure 7. Rayleigh absolute calibration results: LEFT camera (Collection 1)

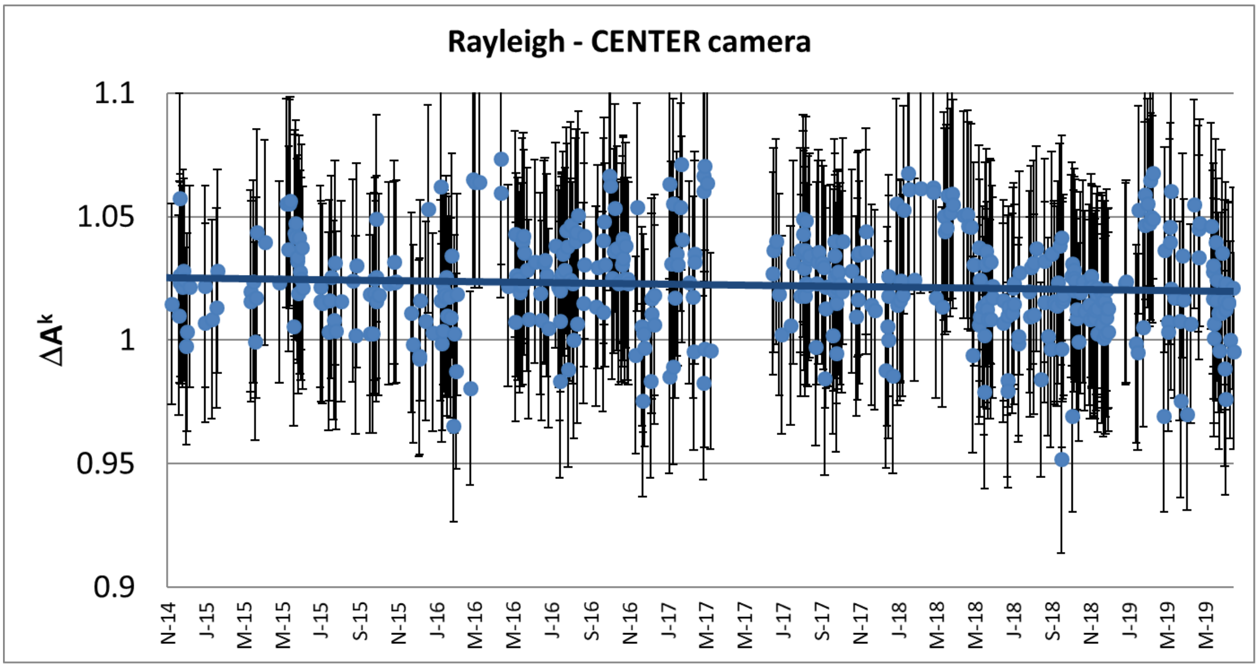

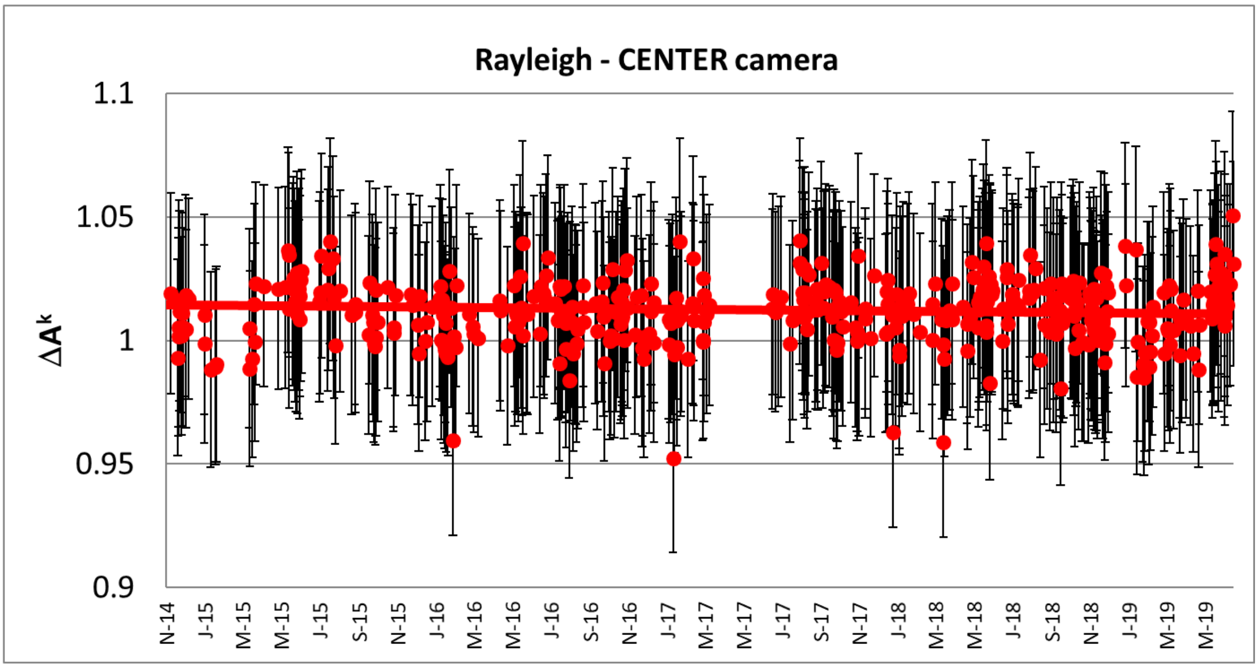

Figure 8. Rayleigh absolute calibration results: CENTER camera (Collection 1)

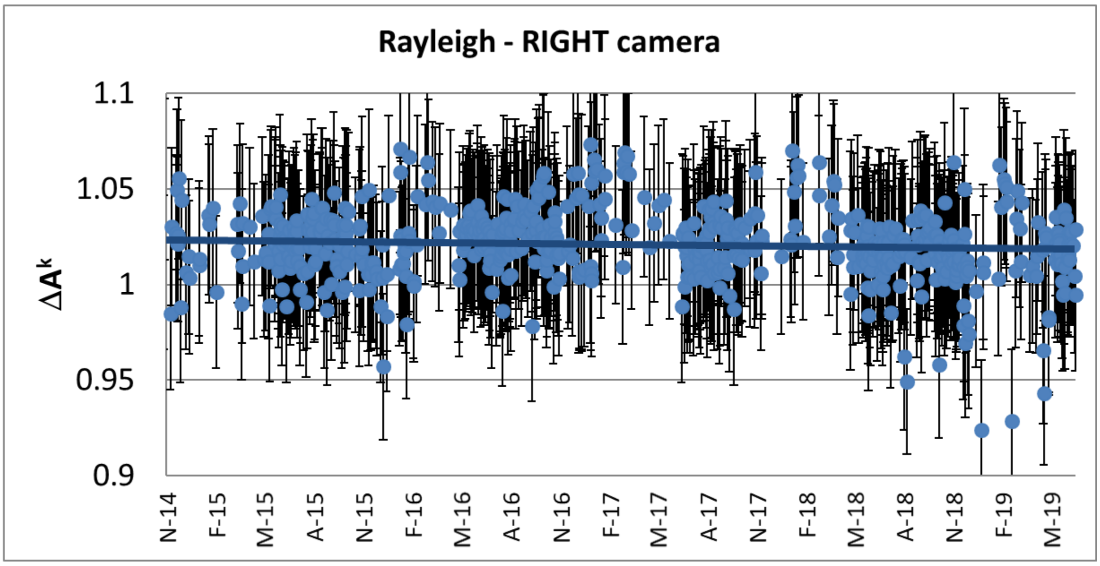

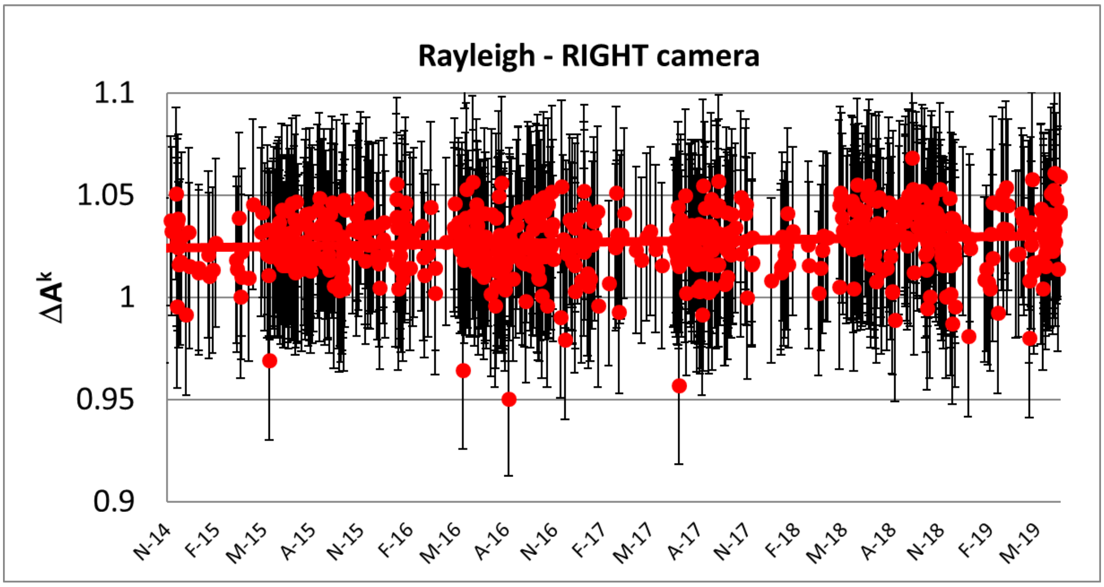

Figure 9. Rayleigh absolute calibration results: RIGHT camera (Collection 1)

1.2.2. Inter-band radiometric accuracy

The inter-band radiometric calibration requirement for PROBA-V specifies a 3 % inter-band accuracy. This requirement is assessed through vicarious calibration over deep convective clouds.

1.2.2.1. Calibration over deep convective clouds (DCC)

Methodology

The DCC approach is an inter-band calibration method. It makes use of bright, thick, high altitude, convective clouds over oceanic sites. Their reflective properties are spectrally flat in visible and near-infrared and the only contributions to the observed signal are from the cloud reflectance, molecular scattering and ozone absorption which can be modelled with a radiative transfer code.
The cloud reflectance in the non-absorbing VNIR bands is mainly sensitive to the cloud optical thickness. The DCC method uses the TOA reflectance in the 'reference' RED band to estimate cloud optical thickness assuming a fixed ice particle model. The derived cloud optical thickness is then used to model using a radiative transfer code the TOA reflectance for the BLUE and NIR band.

The method is not suited for the SWIR band as clouds are no longer spectrally uniform in this spectral region.

Results

The DCC inter-band calibration is defined by reference to the used RED reference band. The average DCC inter-band calibration result per month (from March 2015 to March 2019) is given in Figure 10 for all cameras using the **collection 1 ICP files**.

The DCC calibration results show a decrease in responsivity of the BLUE bands of all cameras, even after May 2017 when the degradation model for BLUE LEFT/CENTER strips was implemented (see 1.2.3.1). Please note that for BLUE RIGHT strip no degradation model is applied as no degradation is observed on the basis of the OSCAR Libya-4 results (see 1.2.1.1). A possible explanation for the trend observed in the DCC BLUE band results, is the increase of responsivity in the RED band as observed in the Libya-4 results for all cameras as well as in the moon calibration results for the CENTER camera. As the BLUE band DCC results, are inter-band calibration results, expressed relatively to the RED band, an increase in responsivity of the RED band (and not for the BLUE band) will result in a decrease of the BLUE band DCC inter-band calibration results.

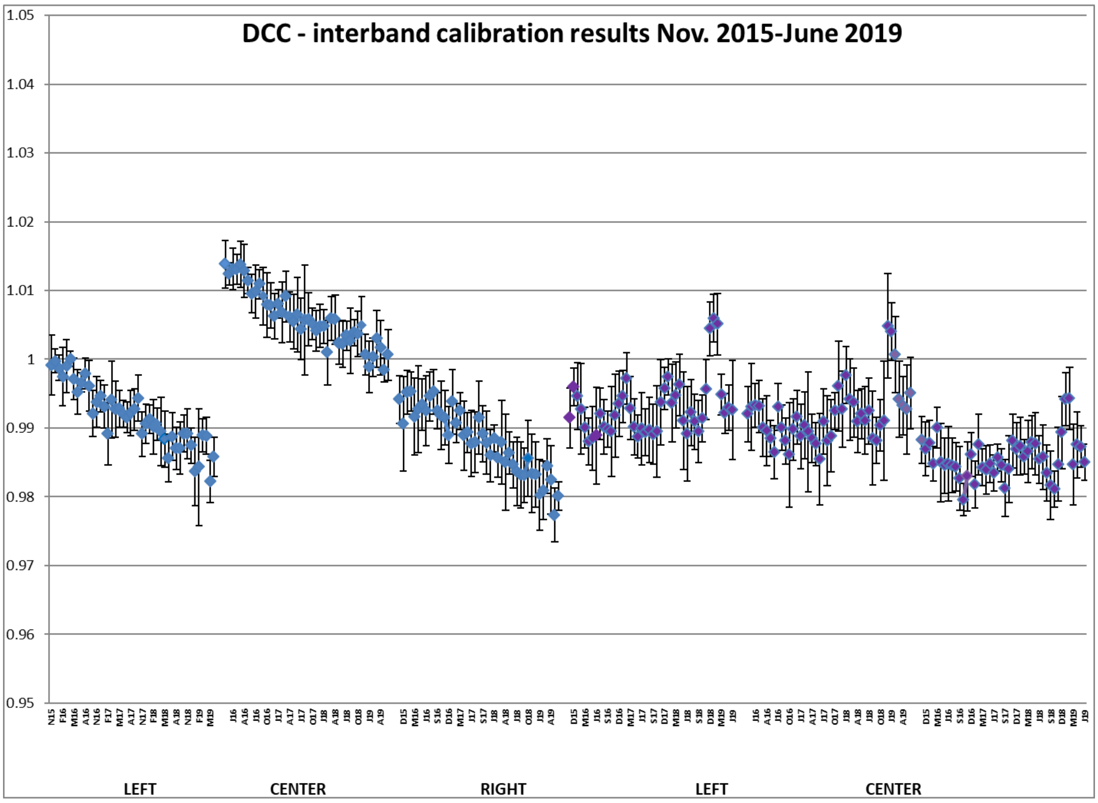

Figure 10. DCC inter-band calibration results: LEFT, CENTER and RIGHT camera

1.2.3. PROBA-V Multi-temporal radiometric accuracy

1.2.3.1. Degradation model

Since October 2018 a degradation model is no longer applied to the SWIR absolute calibration coefficients as the current linear model resulted in an overcorrection of the degradation in the SWIR. Once ICP files are updated for the non-uniformities as quantified on the basis of the yaw maneuver, the Libya-4 desert results will be reprocessed in order to better quantify the degradation for the various SWIR strips and to re-evaluate the degradation model for the SWIR strips to be used in the reprocessing (collection 2).

In Table 1 the applied degradation model correction is given. This linear degradation model is being applied for collection 1 since start of the operational phase (i.e. October 2013). A re-evaluation of the coefficients of the SWIR degradation model was performed in summer 2017. Since Jan 2018 a degradation model is no longer applied to the RIGHT SWIR strips. From October 2018 onwards, absolute calibration coefficients for the SWIR strips are not updated.

Table 1 SWIR degradation model: applied linear trend/month

	Degradation model ICP			
	Start- aug 2017	Sept 2017-Dec 2018	Jan 2018-Sept 2018	Oct 2018-..
SWIR1 LEFT	-0.087	-0.087	-0.087	NA
SWIR2 LEFT	-0.104	-0.104	-0.104	NA
SWIR3 LEFT	-0.097	-0.097	-0.097	NA
SWIR1 CENTER	-0.093	-0.093	-0.093	NA
SWIR2 CENTER	-0.092	-0.092	-0.092	NA
SWIR3 CENTER	-0.086	-0.086	-0.086	NA
SWIR1 RIGHT	-0.106	-0.077	NA	NA
SWIR2 RIGHT	-0.143	-0.122	NA	NA
SWIR3 RIGHT	-0.122	-0.078	NA	NA

A degradation model is used to update the absolute calibration coefficients of the LEFT and RIGHT BLUE since May 2017. A re-evaluation of the coefficients of the degradation model was performed in summer 2017. Since then no changes have been made to the model. In Table 2 the coefficients are given.

Table 2 Degradation model BLUE LEFT and CENTER camera: applied linear trend/month

STRIP	Linear trend/month (%)	
	Degradation model ICP May 2017-aug 2017	Degradation model ICP since sept 2017
BLUE LEFT	-0.028	-0.036
BLUE CENTER	-0.011	-0.034

1.2.3.2. Lunar calibration

The Lunar calibration results for the VNIR CENTER camera bands, normalised to June 2013, are given in Figure 11. The results are given based on the **collection 1 ICP** files.

Over the entire mission the BLUE band lunar calibration results show a decreasing trend which is more pronounced in the first years when the BLUE band degradation model was not yet in place (implemented since May 2017). the LEFT and CENTER absolute calibration coefficients for the BLUE band are monthly updated following a linear degradation model (see section 1.2.3). The slight degradation observed in the BLUE band desert results for LEFT and CENTER camera are probably due to degradation in the first years for which a degradation model was not yet in place.

The DCC the RED and NIR lunar calibration results show an increase. Please note that for the November till February 2019 results the NIR band increase is probably caused by the increased temperature due to absence of sun bathing.

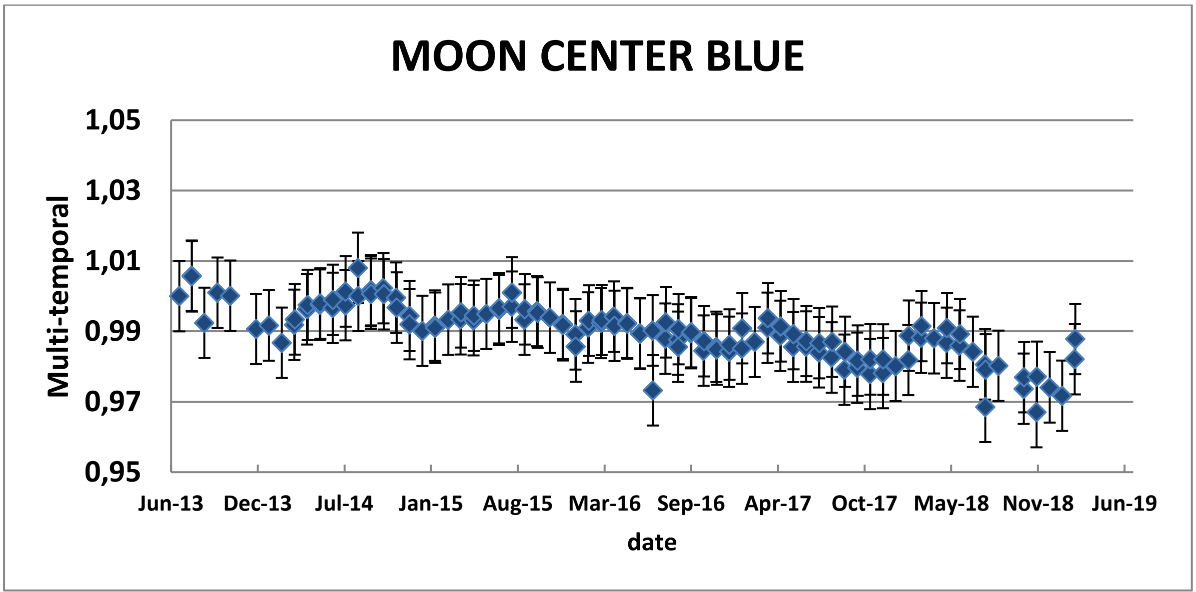

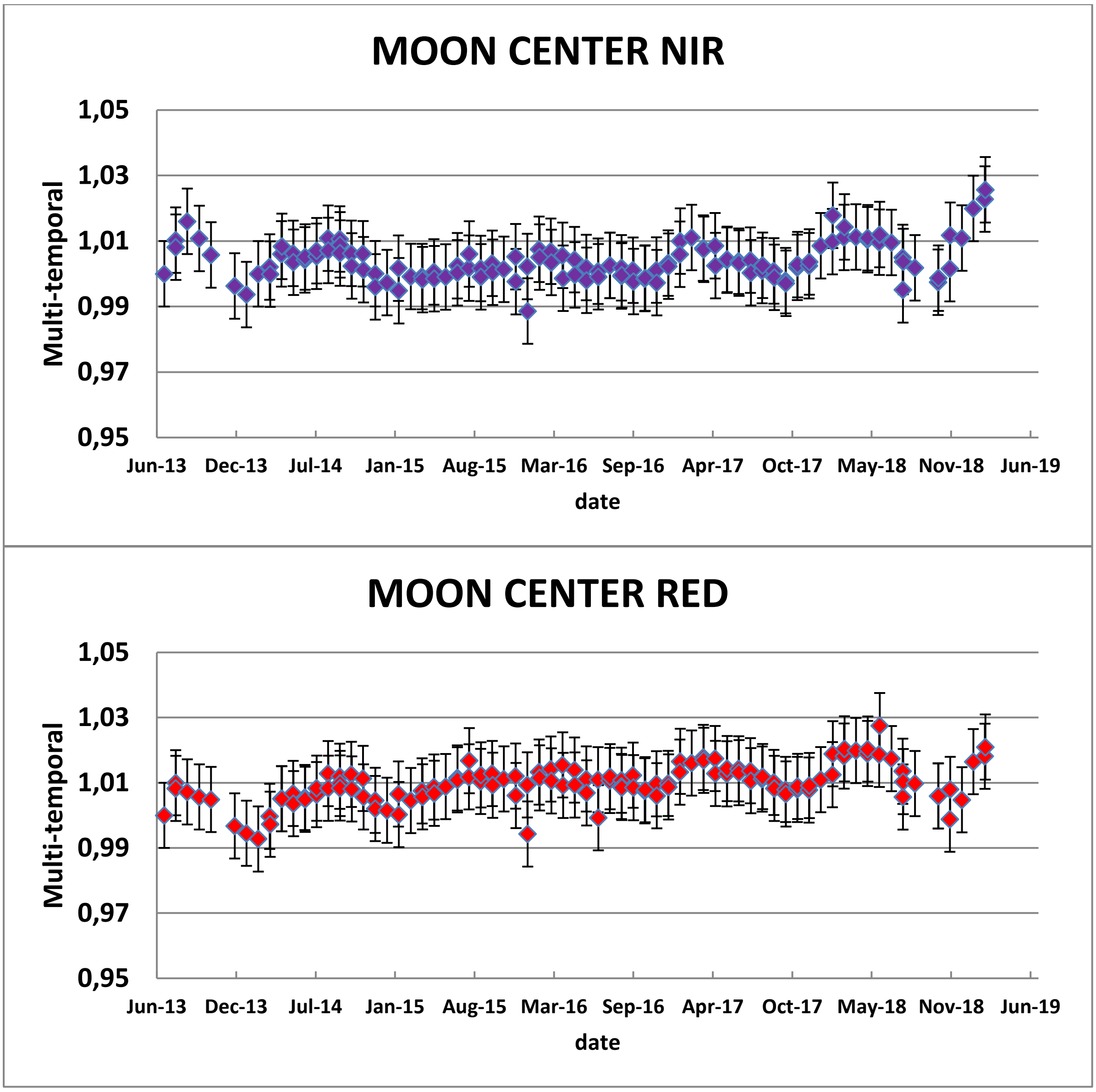

Figure 11. Lunar Calibration results CENTER camera normalised to June 2013 (collection 1 ICP files)

1.2.3.3. Libya-4 VS Moon

As mentioned in previous report degradation trends observed in the Lunar calibration results for the center SWIR2 strip are less significant than these observed in the desert calibration results. In the frame of the ESA's 'Lunar Irradiance Measurements of the Moon' project VITO is working on an improved lunar model. A reprocessing of the PROBA-V lunar calibration results based on the improved model is foreseen for the near future. It is expected that this will give us a better insight in the actual degradation trend.

1.3. Dark current

1.3.1. Methodology

- Monthly difference plots:
    - All dark current results obtained during a period of one month for observations performed with a long integration time are averaged per pixel. This gives for each pixel the monthly averaged dark current, expressed **in LSB/s**, and its standard deviation.
    - The dark current results and its standard deviation expressed in LSB/s are converted to **LSB** using a maximum Integration Time for nominal acquisitions. For VNIR strips **0.006s** is used. For SWIR strips **0.02s.**
    - The differences between months (i.e. Month3-Month2, Month2-Month1) are calculated. This is done for both the dark current and the stdev. Differences are visualized in plots in blue the dark current difference in LSB is plotted, in red the standard deviation difference. This latter is an indicator of changes in the dark current noise between months.

As mentioned in the previous quarterly report (IQR#005) the integration time used for the SWIR dark current acquisitions has been decreased from 3s to 0.2 s since 2015.

1.3.2. VNIR results

Monthly difference plots for VNIR dark currents are given Figure 12, *Figure 13* and *Figure 14* for respectively LEFT, CENTER and RIGHT camera.

Dark current differences for the VNIR bands are well below 1 DN, except for a very few outliners.

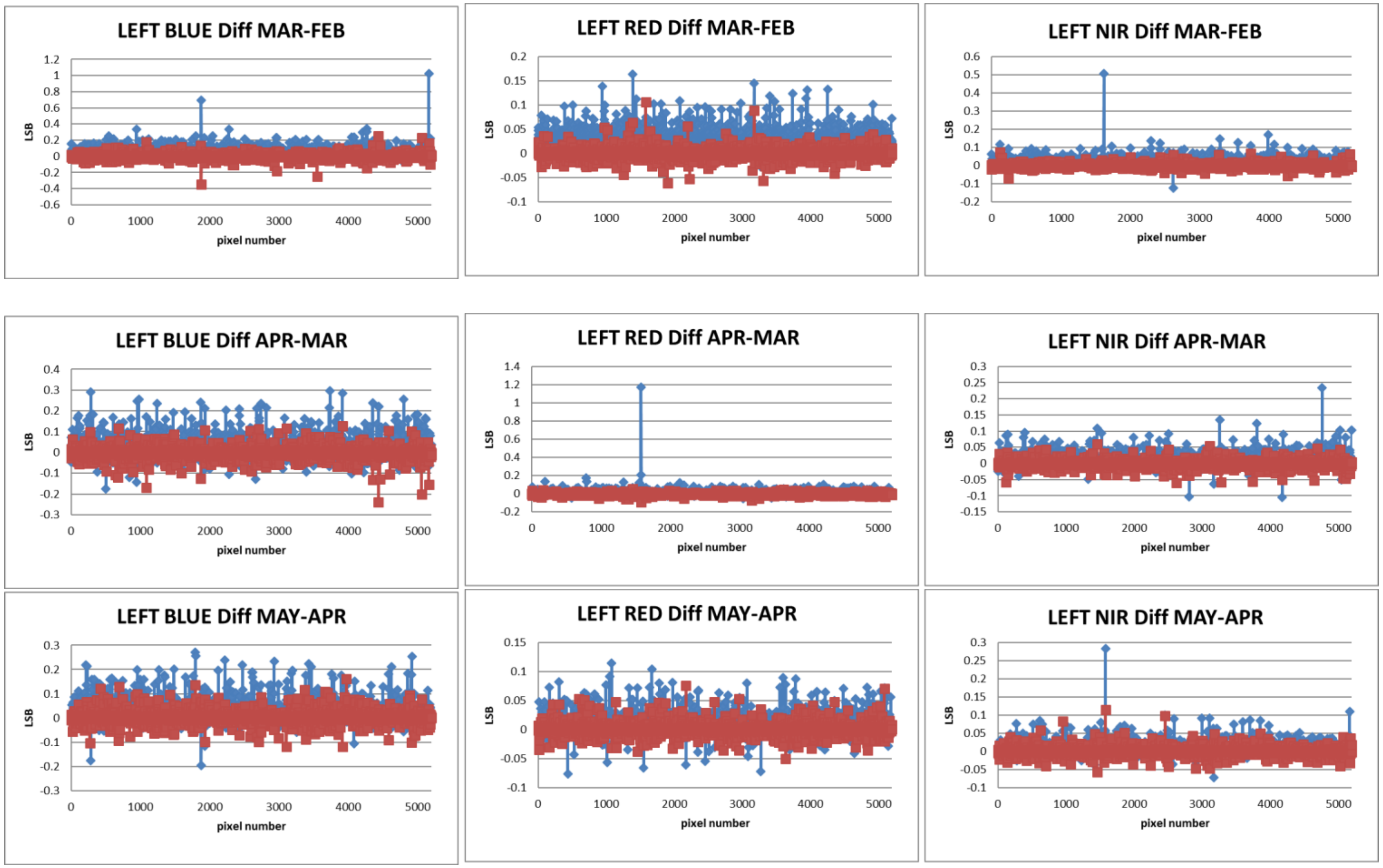

Figure 12. LEFT camera VNIR: Monthly difference (FEB2019-MAY2019) in dark current (Blue) and standard deviation (Red) of the monthly averaged results.

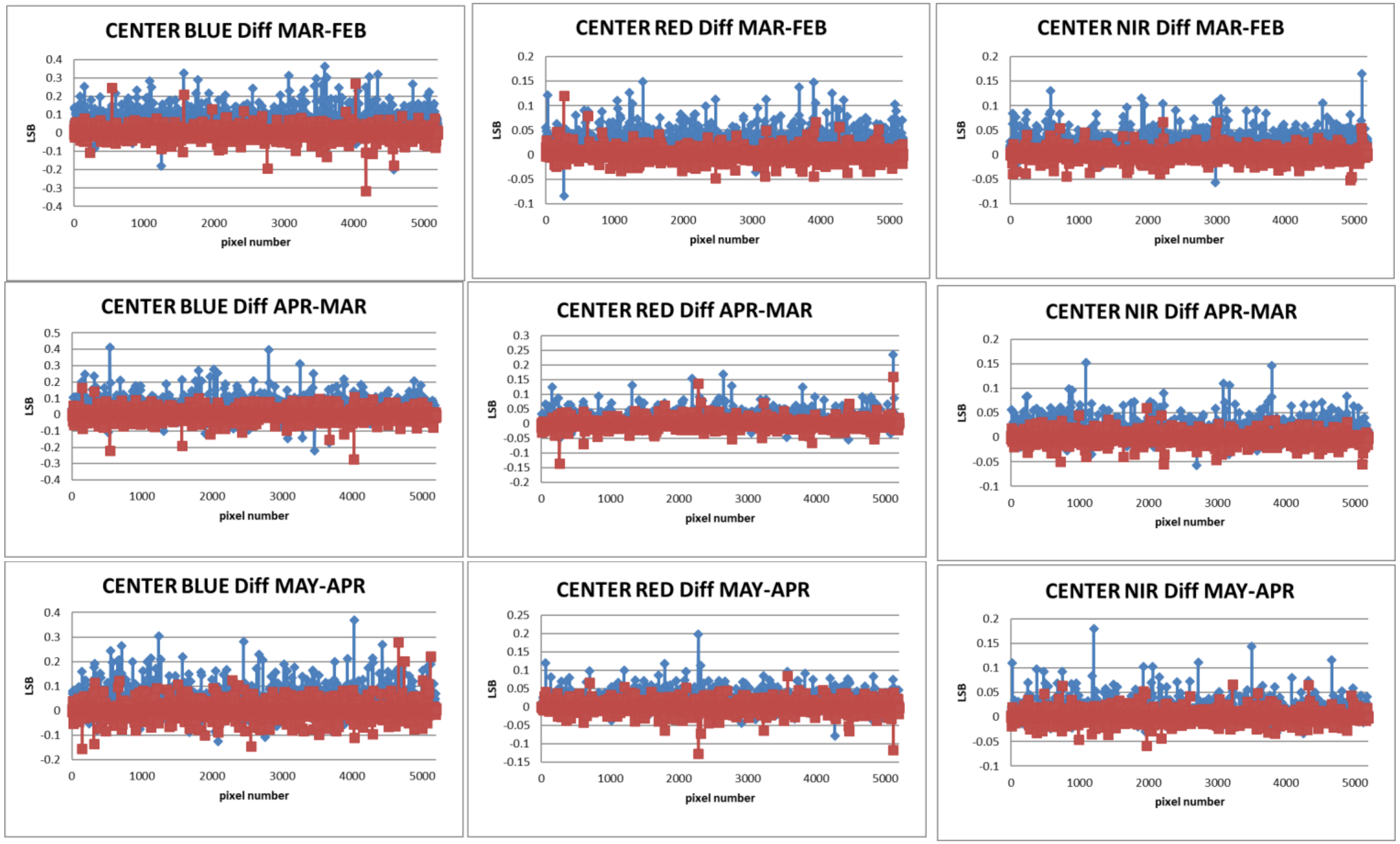

*Figure 13. CENTER camera VNIR: Monthly difference (*FEB2019-MAY2019*) in dark current (Blue) and standard deviation (Red) of the monthly averaged results.*

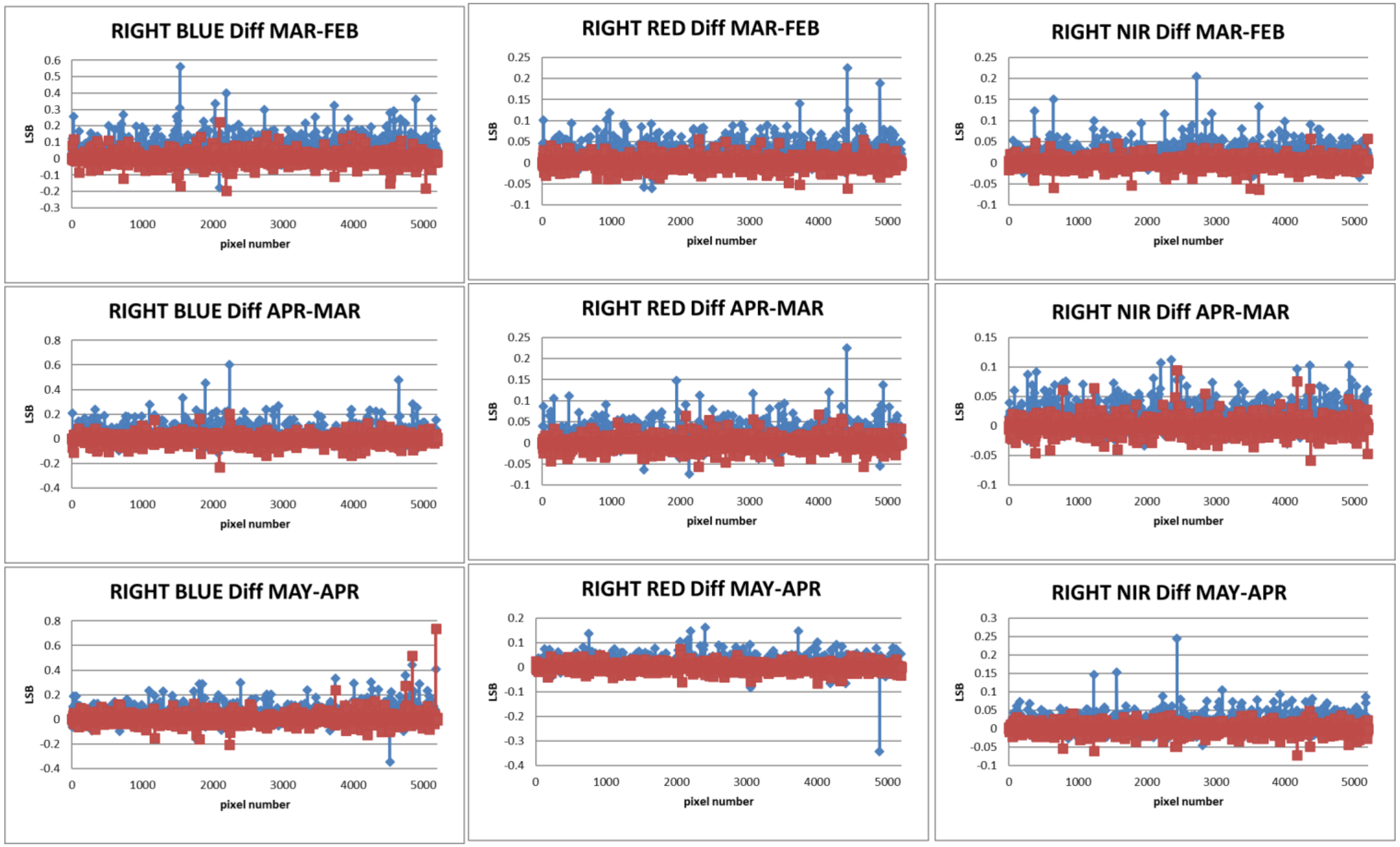

*Figure 14. RIGHT camera VNIR: Monthly difference (*NOV 2018-FEB2019*) in dark current (Blue) and standard deviation (Red) of the monthly averaged results.*

1.3.3. SWIR results

Monthly difference plots for SWIR dark currents are given in Figure 15, Figure 16 and Figure 17 for respectively LEFT, CENTER and RIGHT camera.

A dark current outlier analysis is performed for pixels having for at least one month a dark current expressed in LSB larger than the DC THRESHOLD. This DC THRESHOLD is set to 4 LSB. For those pixels the following dark current pixel statuses are given:

- Both monthly differences > 4 LSB ? **Quality is "H DC BAD"**
- One monthly difference > 4 LSB ? **Quality is "H DC NOK"**.
- Both monthly differences < 4 LSB ? **Quality is "H DC OK"**

In *Table 3*

JAN-FEB-MAR						FEB-MAR-APR						MAR-APR-MAY					
SWIR1		SWIR2		SWIR3		SWIR1		SWIR2		SWIR3		SWIR1		SWIR2		SWIR3	
3	H DC BAD	33	H DC NOK	46 pixels	H DC BAD	3	H DC BAD	959	H DC BAD	20	H DC BAD	39	H DC BAD	839	H DC BAD	82	H DC BAD
28	H DC BAD	77	H DC NOK	570 pixels	H DC NOK	28	H DC BAD	33	H DC NOK	75	H DC BAD	3	H DC NOK	717	H DC NOK	370	H DC BAD
298	H DC BAD	116	H DC NOK	398pixels	H DC OK	39	H DC BAD	77	H DC NOK	90	H DC BAD	28	H DC NOK	959	H DC NOK	513	H DC BAD
345	H DC BAD	174	H DC NOK			298	H DC BAD	116	H DC NOK	115	H DC BAD	75	H DC NOK	967	H DC NOK	824	H DC BAD
956	H DC BAD	192	H DC NOK			345	H DC BAD	174	H DC NOK	121	H DC BAD	290	H DC NOK	388 pixels	H DC OK	966	H DC BAD
996	H DC BAD	211	H DC NOK			956	H DC BAD	192	H DC NOK	173	H DC BAD	298	H DC NOK			20	H DC NOK
39	H DC NOK	272	H DC NOK			75	H DC NOK	211	H DC NOK	178	H DC BAD	323	H DC NOK			75	H DC NOK
78	H DC NOK	284	H DC NOK			78	H DC NOK	272	H DC NOK	198	H DC BAD	345	H DC NOK			76	H DC NOK
104	H DC NOK	294	H DC NOK			104	H DC NOK	284	H DC NOK	276	H DC BAD	823	H DC NOK			90	H DC NOK
120	H DC NOK	305	H DC NOK			120	H DC NOK	294	H DC NOK	336	H DC BAD	928	H DC NOK			105	H DC NOK
187	H DC NOK	311	H DC NOK			187	H DC NOK	305	H DC NOK	362	H DC BAD	951	H DC NOK			115	H DC NOK
222	H DC NOK	333	H DC NOK			222	H DC NOK	311	H DC NOK	370	H DC BAD	956	H DC NOK			121	H DC NOK
290	H DC NOK	362	H DC NOK			290	H DC NOK	333	H DC NOK	419	H DC BAD	252 pixels	H DC OK			173	H DC NOK
338	H DC NOK	366	H DC NOK			338	H DC NOK	362	H DC NOK	470	H DC BAD					178	H DC NOK
352	H DC NOK	397	H DC NOK			352	H DC NOK	366	H DC NOK	564	H DC BAD					198	H DC NOK
365	H DC NOK	556	H DC NOK			365	H DC NOK	397	H DC NOK	568	H DC BAD					276	H DC NOK
385	H DC NOK	578	H DC NOK			385	H DC NOK	556	H DC NOK	591	H DC BAD					336	H DC NOK
425	H DC NOK	580	H DC NOK			425	H DC NOK	580	H DC NOK	750	H DC BAD					362	H DC NOK
575	H DC NOK	702	H DC NOK			575	H DC NOK	702	H DC NOK	753	H DC BAD					400	H DC NOK
626	H DC NOK	711	H DC NOK			644	H DC NOK	711	H DC NOK	761	H DC BAD					419	H DC NOK
644	H DC NOK	778	H DC NOK			646	H DC NOK	778	H DC NOK	804	H DC BAD					470	H DC NOK
646	H DC NOK	859	H DC NOK			678	H DC NOK	839	H DC NOK	818	H DC BAD					548	H DC NOK
678	H DC NOK	863	H DC NOK			823	H DC NOK	859	H DC NOK	824	H DC BAD					564	H DC NOK
892	H DC NOK	873	H DC NOK			892	H DC NOK	863	H DC NOK	856	H DC BAD					568	H DC NOK
950	H DC NOK	922	H DC NOK			928	H DC NOK	873	H DC NOK	897	H DC BAD					591	H DC NOK
957	H DC NOK	959	H DC NOK			950	H DC NOK	922	H DC NOK	957	H DC BAD					641	H DC NOK
974	H DC NOK	333 pixels	H DC OK			957	H DC NOK	350 pixels	H DC OK	966	H DC BAD					750	H DC NOK
987	H DC NOK					974	H DC NOK			998	H DC BAD					753	H DC NOK
211 pixels	H DC OK					987	H DC NOK			588 pixels	H DC NOK					761	H DC NOK
						996	H DC NOK			394pixels	H DC OK					804	H DC NOK
						226 pixels	H DC OK									818	H DC NOK
																856	H DC NOK
																897	H DC NOK
																910	H DC NOK
																957	H DC NOK
																998	H DC NOK
																924pixels	H DC OK

Table 3. LEFT SWIR dark current pixel outliers (ID L1A).

, *Table 4*,*Table 5* the resulting SWIR dark current status during the last 3 months is reported for respectively LEFT, CENTER and RIGHT camera.

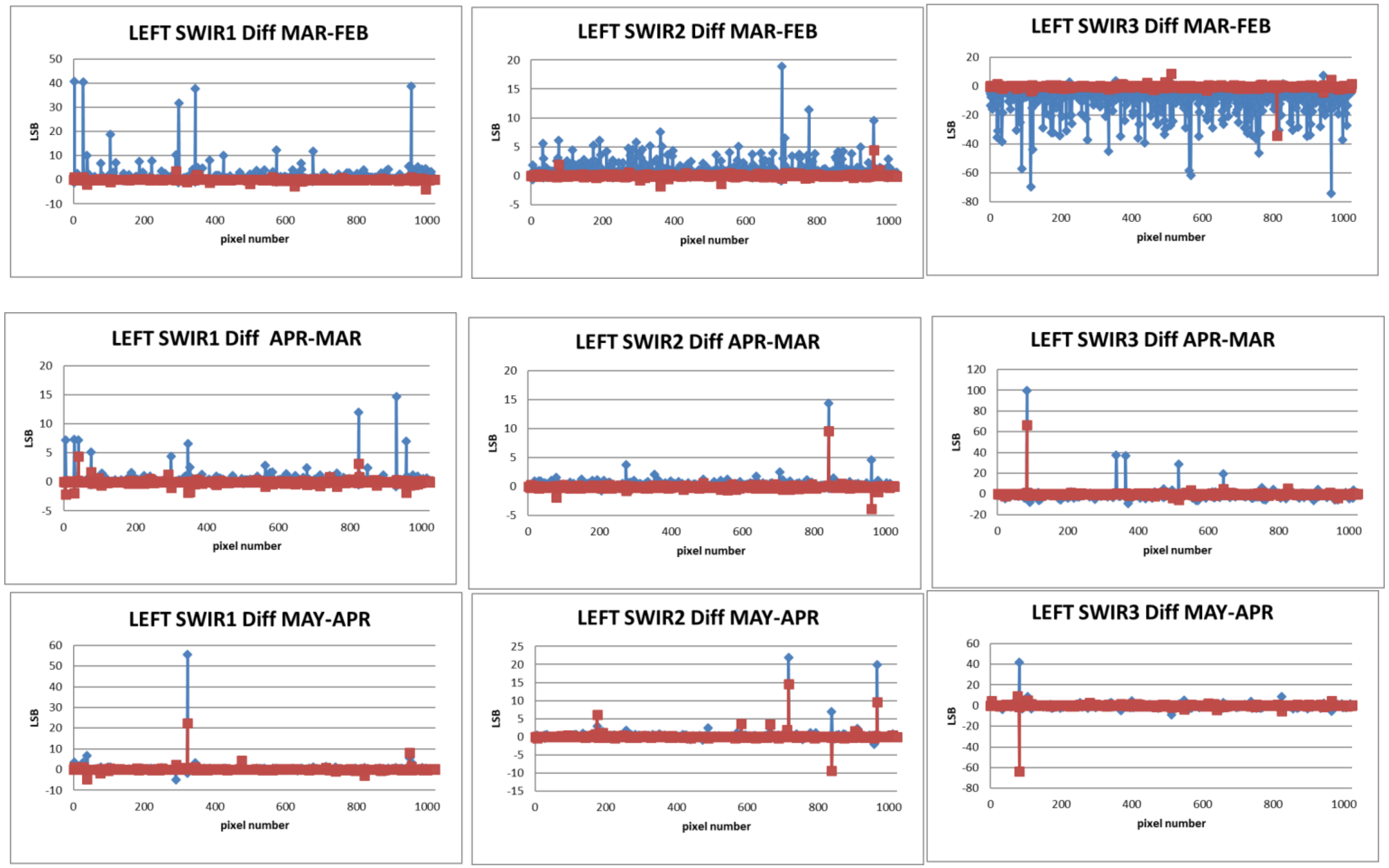

Figure 15. LEFT camera SWIR: Monthly difference (FEB2019-MAY2019) in dark current (Blue) and standard deviation (Red) of the monthly averaged results.

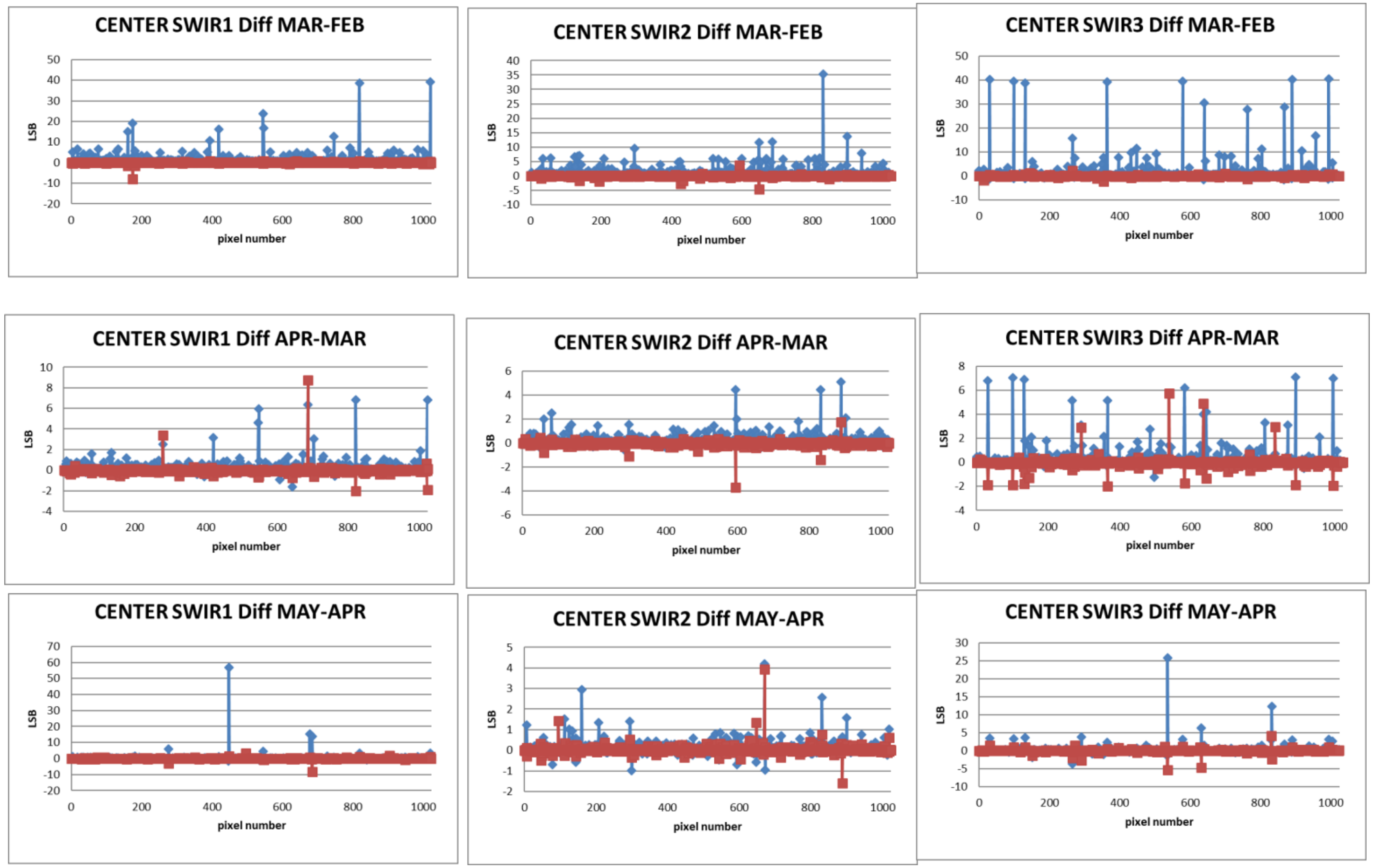

Figure 16. CENTER camera SWIR: Monthly difference (FEB2019-MAY2019) in dark current (Blue) and standard deviation (Red) of the monthly averaged results.

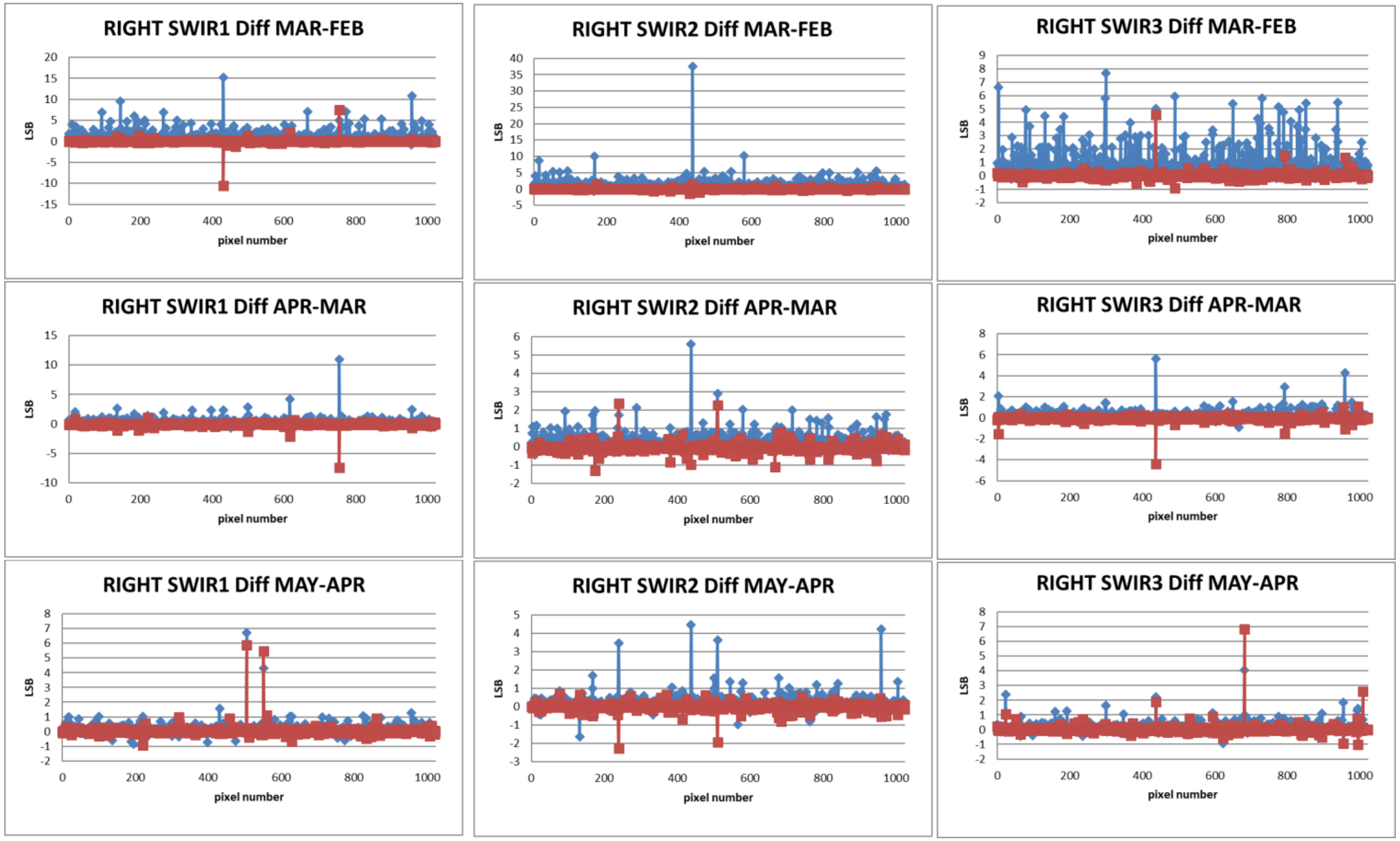

Figure 17. RIGHT camera SWIR: Monthly difference (FEB2019-MAY2019) in dark current (Blue) and standard deviation (Red) of the monthly averaged results.

JAN-FEB-MAR						FEB-MAR-APR						MAR-APR-MAY					
SWIR1		SWIR2		SWIR3		SWIR1		SWIR2		SWIR3		SWIR1		SWIR2		SWIR3	
3	H DC BAD	33	H DC NOK	46 pixels	H DC BAD	3	H DC BAD	959	H DC BAD	20	H DC BAD	39	H DC BAD	839	H DC BAD	82	H DC BAD
28	H DC BAD	77	H DC NOK	570 pixels	H DC NOK	28	H DC BAD	33	H DC NOK	75	H DC BAD	3	H DC NOK	717	H DC NOK	370	H DC BAD
298	H DC BAD	116	H DC NOK	398pixels	H DC OK	39	H DC BAD	77	H DC NOK	90	H DC BAD	28	H DC NOK	959	H DC NOK	513	H DC BAD
345	H DC BAD	174	H DC NOK			298	H DC BAD	116	H DC NOK	115	H DC BAD	75	H DC NOK	967	H DC NOK	824	H DC BAD
956	H DC BAD	192	H DC NOK			345	H DC BAD	174	H DC NOK	121	H DC BAD	290	H DC NOK	388 pixels	H DC OK	966	H DC BAD
996	H DC BAD	211	H DC NOK			956	H DC BAD	192	H DC NOK	173	H DC BAD	298	H DC NOK			20	H DC NOK
39	H DC NOK	272	H DC NOK			75	H DC NOK	211	H DC NOK	178	H DC BAD	323	H DC NOK			75	H DC NOK
78	H DC NOK	284	H DC NOK			78	H DC NOK	272	H DC NOK	198	H DC BAD	345	H DC NOK			76	H DC NOK
104	H DC NOK	294	H DC NOK			104	H DC NOK	284	H DC NOK	276	H DC BAD	823	H DC NOK			90	H DC NOK
120	H DC NOK	305	H DC NOK			120	H DC NOK	294	H DC NOK	336	H DC BAD	928	H DC NOK			105	H DC NOK
187	H DC NOK	311	H DC NOK			187	H DC NOK	305	H DC NOK	362	H DC BAD	951	H DC NOK			115	H DC NOK
222	H DC NOK	333	H DC NOK			222	H DC NOK	311	H DC NOK	370	H DC BAD	956	H DC NOK			121	H DC NOK
290	H DC NOK	362	H DC NOK			290	H DC NOK	333	H DC NOK	419	H DC BAD	252 pixels	H DC OK			173	H DC NOK
338	H DC NOK	366	H DC NOK			338	H DC NOK	362	H DC NOK	470	H DC BAD					178	H DC NOK
352	H DC NOK	397	H DC NOK			352	H DC NOK	366	H DC NOK	564	H DC BAD					198	H DC NOK
365	H DC NOK	556	H DC NOK			365	H DC NOK	397	H DC NOK	568	H DC BAD					276	H DC NOK
385	H DC NOK	578	H DC NOK			385	H DC NOK	556	H DC NOK	591	H DC BAD					336	H DC NOK
425	H DC NOK	580	H DC NOK			425	H DC NOK	580	H DC NOK	750	H DC BAD					362	H DC NOK
575	H DC NOK	702	H DC NOK			575	H DC NOK	702	H DC NOK	753	H DC BAD					400	H DC NOK
626	H DC NOK	711	H DC NOK			644	H DC NOK	711	H DC NOK	761	H DC BAD					419	H DC NOK
644	H DC NOK	778	H DC NOK			646	H DC NOK	778	H DC NOK	804	H DC BAD					470	H DC NOK
646	H DC NOK	859	H DC NOK			678	H DC NOK	839	H DC NOK	818	H DC BAD					548	H DC NOK
678	H DC NOK	863	H DC NOK			823	H DC NOK	859	H DC NOK	824	H DC BAD					564	H DC NOK
892	H DC NOK	873	H DC NOK			892	H DC NOK	863	H DC NOK	856	H DC BAD					568	H DC NOK
950	H DC NOK	922	H DC NOK			928	H DC NOK	873	H DC NOK	897	H DC BAD					591	H DC NOK
957	H DC NOK	959	H DC NOK			950	H DC NOK	922	H DC NOK	957	H DC BAD					641	H DC NOK
974	H DC NOK	333 pixels	H DC OK			957	H DC NOK	350 pixels	H DC OK	966	H DC BAD					750	H DC NOK
987	H DC NOK					974	H DC NOK			998	H DC BAD					753	H DC NOK
211 pixels	H DC OK					987	H DC NOK			588 pixels	H DC NOK					761	H DC NOK
						996	H DC NOK			394pixels	H DC OK					804	H DC NOK
						226 pixels	H DC OK									818	H DC NOK
																856	H DC NOK
																897	H DC NOK
																910	H DC NOK
																957	H DC NOK
																998	H DC NOK
																924pixels	H DC OK

Table 3. LEFT SWIR dark current pixel outliers (ID L1A).

CENTER																	
JAN-FEB-MAR						FEB-MAR-APR						MAR-APR_MAY					
SWIR1		SWIR2		SWIR3		SWIR1		SWIR2		SWIR3		SWIR1		SWIR2		SWIR3	
175	H DC BAD	34	H DC NOK	30	H DC NOK	545	H DC BAD	831	H DC BAD	30	H DC BAD	545	H DC BAD	593	H DC NOK	632	H DC BAD
5	H DC NOK	57	H DC NOK	99	H DC NOK	547	H DC BAD	34	H DC NOK	99	H DC BAD	685	H DC BAD	671	H DC NOK	30	H DC NOK
18	H DC NOK	125	H DC NOK	131	H DC NOK	819	H DC BAD	57	H DC NOK	131	H DC BAD	277	H DC NOK	831	H DC NOK	99	H DC NOK
35	H DC NOK	134	H DC NOK	152	H DC NOK	1021	H DC BAD	125	H DC NOK	266	H DC BAD	448	H DC NOK	888	H DC NOK	131	H DC NOK
51	H DC NOK	138	H DC NOK	252	H DC NOK	5	H DC NOK	134	H DC NOK	364	H DC BAD	547	H DC NOK	331pixels	H DC OK	266	H DC NOK
54	H DC NOK	208	H DC NOK	266	H DC NOK	18	H DC NOK	138	H DC NOK	579	H DC BAD	678	H DC NOK			364	H DC NOK
77	H DC NOK	266	H DC NOK	272	H DC NOK	35	H DC NOK	208	H DC NOK	640	H DC BAD	819	H DC NOK			536	H DC NOK
128	H DC NOK	295	H DC NOK	326	H DC NOK	51	H DC NOK	266	H DC NOK	890	H DC BAD	1021	H DC NOK			579	H DC NOK
133	H DC NOK	419	H DC NOK	348	H DC NOK	54	H DC NOK	295	H DC NOK	994	H DC BAD	264pixels	H DC OK			640	H DC NOK
161	H DC NOK	425	H DC NOK	354	H DC NOK	77	H DC NOK	419	H DC NOK	152	H DC NOK					832	H DC NOK
181	H DC NOK	518	H DC NOK	364	H DC NOK	128	H DC NOK	425	H DC NOK	252	H DC NOK					890	H DC NOK
253	H DC NOK	533	H DC NOK	397	H DC NOK	133	H DC NOK	518	H DC NOK	272	H DC NOK					994	H DC NOK
316	H DC NOK	553	H DC NOK	432	H DC NOK	161	H DC NOK	533	H DC NOK	326	H DC NOK					166pixels	H DC OK
350	H DC NOK	596	H DC NOK	448	H DC NOK	175	H DC NOK	553	H DC NOK	348	H DC NOK						
387	H DC NOK	599	H DC NOK	476	H DC NOK	181	H DC NOK	593	H DC NOK	354	H DC NOK						
394	H DC NOK	634	H DC NOK	504	H DC NOK	253	H DC NOK	596	H DC NOK	397	H DC NOK						
419	H DC NOK	646	H DC NOK	579	H DC NOK	316	H DC NOK	599	H DC NOK	432	H DC NOK						
545	H DC NOK	648	H DC NOK	640	H DC NOK	350	H DC NOK	634	H DC NOK	448	H DC NOK						
547	H DC NOK	649	H DC NOK	644	H DC NOK	387	H DC NOK	646	H DC NOK	476	H DC NOK						
566	H DC NOK	655	H DC NOK	682	H DC NOK	394	H DC NOK	648	H DC NOK	504	H DC NOK						
641	H DC NOK	669	H DC NOK	697	H DC NOK	419	H DC NOK	649	H DC NOK	632	H DC NOK						
671	H DC NOK	684	H DC NOK	716	H DC NOK	566	H DC NOK	655	H DC NOK	644	H DC NOK						
728	H DC NOK	687	H DC NOK	729	H DC NOK	641	H DC NOK	669	H DC NOK	682	H DC NOK						
747	H DC NOK	718	H DC NOK	763	H DC NOK	671	H DC NOK	684	H DC NOK	697	H DC NOK						
792	H DC NOK	789	H DC NOK	794	H DC NOK	685	H DC NOK	687	H DC NOK	716	H DC NOK						
802	H DC NOK	807	H DC NOK	804	H DC NOK	728	H DC NOK	718	H DC NOK	729	H DC NOK						
819	H DC NOK	821	H DC NOK	868	H DC NOK	747	H DC NOK	789	H DC NOK	763	H DC NOK						
845	H DC NOK	831	H DC NOK	890	H DC NOK	792	H DC NOK	807	H DC NOK	794	H DC NOK						
900	H DC NOK	900	H DC NOK	917	H DC NOK	802	H DC NOK	821	H DC NOK	804	H DC NOK						
908	H DC NOK	941	H DC NOK	938	H DC NOK	845	H DC NOK	888	H DC NOK	868	H DC NOK						
914	H DC NOK	1002	H DC NOK	957	H DC NOK	900	H DC NOK	900	H DC NOK	917	H DC NOK						
916	H DC NOK	273pixels	H DC OK	994	H DC NOK	908	H DC NOK	941	H DC NOK	938	H DC NOK						
933	H DC NOK			1005	H DC NOK	914	H DC NOK	1002	H DC NOK	957	H DC NOK						
985	H DC NOK			126pixels	H DC OK	916	H DC NOK	293pixels	H DC OK	1005	H DC NOK						
1001	H DC NOK					933	H DC NOK			136pixels	H DC OK						
1021	H DC NOK					985	H DC NOK										
215pixels	H DC OK					1001	H DC NOK										
						224pixels	H DC OK										

Table 4. CENTER SWIR dark current pixel outliers (ID L1A)

RIGHT

JAN-FEB-MAR					
431	H DC BAD	438	H DC BAD	490	H DC BAD
10	H DC NOK	14	H DC BAD	3	H DC NOK
92	H DC NOK	32	H DC BAD	78	H DC NOK
116	H DC NOK	53	H DC BAD	131	H DC NOK
144	H DC NOK	71	H DC BAD	183	H DC NOK
162	H DC NOK	92	H DC BAD	297	H DC NOK
183	H DC NOK	167	H DC BAD	300	H DC NOK
195	H DC NOK	421	H DC BAD	437	H DC NOK
212	H DC NOK	470	H DC BAD	650	H DC NOK
213	H DC NOK	545	H DC BAD	719	H DC NOK
264	H DC NOK	566	H DC BAD	730	H DC NOK
302	H DC NOK	580	H DC BAD	777	H DC NOK
342	H DC NOK	689	H DC BAD	790	H DC NOK
398	H DC NOK	797	H DC BAD	810	H DC NOK
424	H DC NOK	815	H DC BAD	834	H DC NOK
666	H DC NOK	893	H DC BAD	852	H DC NOK
713	H DC NOK	946	H DC BAD	939	H DC NOK
755	H DC NOK	489pixels	H DC OK	361pixels	H DC OK
774	H DC NOK				
783	H DC NOK				
825	H DC NOK				
873	H DC NOK				
877	H DC NOK				
928	H DC NOK				
957	H DC NOK				
963	H DC NOK				
985	H DC NOK				
1005	H DC NOK				
422 pixels	H DC OK				

FEB-MAR-APR					
755	H DC BAD	438	H DC BAD	437	H DC BAD
10	H DC NOK	14	H DC BAD	3	H DC NOK
92	H DC NOK	32	H DC BAD	78	H DC NOK
116	H DC NOK	53	H DC BAD	131	H DC NOK
144	H DC NOK	71	H DC BAD	183	H DC NOK
162	H DC NOK	92	H DC BAD	297	H DC NOK
183	H DC NOK	167	H DC BAD	300	H DC NOK
195	H DC NOK	421	H DC BAD	490	H DC NOK
212	H DC NOK	470	H DC BAD	650	H DC NOK
213	H DC NOK	545	H DC BAD	719	H DC NOK
264	H DC NOK	580	H DC BAD	730	H DC NOK
302	H DC NOK	797	H DC BAD	777	H DC NOK
342	H DC NOK	815	H DC BAD	790	H DC NOK
398	H DC NOK	893	H DC BAD	810	H DC NOK
424	H DC NOK	946	H DC BAD	834	H DC NOK
431	H DC NOK	532pixels	H DC OK	852	H DC NOK
617	H DC NOK			939	H DC NOK
666	H DC NOK			959	H DC NOK
774	H DC NOK			388pixels	H DC OK
783	H DC NOK				
825	H DC NOK				
873	H DC NOK				
928	H DC NOK				
957	H DC NOK				
963	H DC NOK				
985	H DC NOK				
1005	H DC NOK				
450pixels	H DC OK				

MAR-APR-MAY					
506	H DC NOK	438	H DC BAD	437	H DC NOK
552	H DC NOK	959	H DC BAD	682	H DC NOK
617	H DC NOK	564pixels	H DC OK	959	H DC NOK
755	H DC NOK			414pixels	H DC OK
488pixels	H DC OK				

Table 5. RIGHT SWIR dark current pixel outliers (ID L1A)

1.4. Yaw manoeuvre: Low Frequency Equalisation

In previous quarterly report the retrieval of the non-uniformity correction coefficients based on the yaw manoeuvre data has been described. Before updating the ICP files on the basis of the yaw-based equalization corrections, an assessment is made on the impact of the corrections on actual images taken over relatively uniform desert sites. To this end a visual comparison is made of the scene (non)uniformity after application of the old (i.e. current) ICP file and though application of ICP file for which the equalization coefficients have been updated using the yaw-maneuver results. Furthermore it is evaluated if only a correction for Low frequency (LF) variation or a correction for both LF and HF (high frequency as striping) is most effective The visual assessments are given in *Figure 18* till *Figure 23*. Visual analyses indicate a clear improvement of the non-uniformities in the scene, both for low and high frequency variations. The operational ICP files will now be updated to include the yaw-based LF and HF corrections of the equalization coefficients.

1.4.1. Left Camera

(Update to LF equalisation)

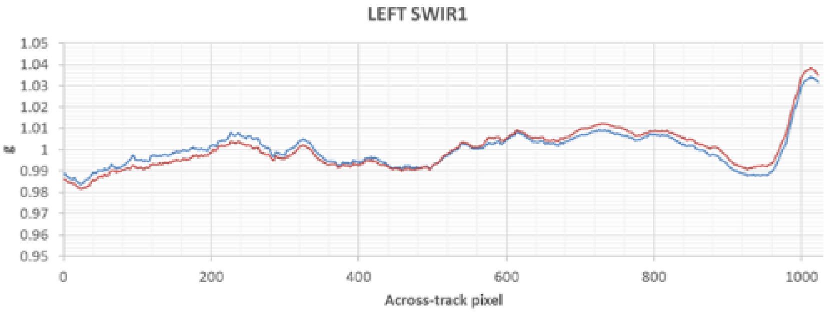

(Old)

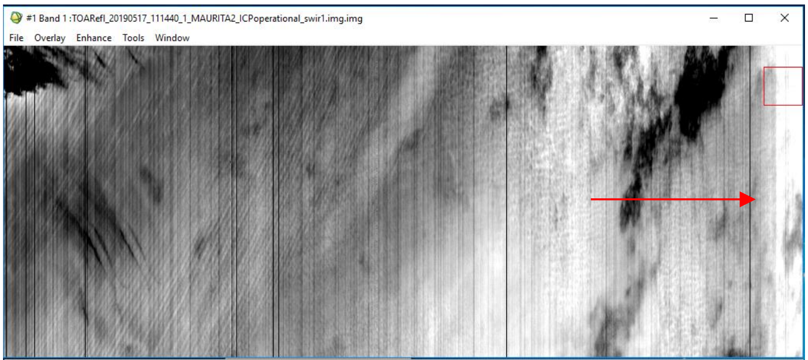

(Update LF equalisation)

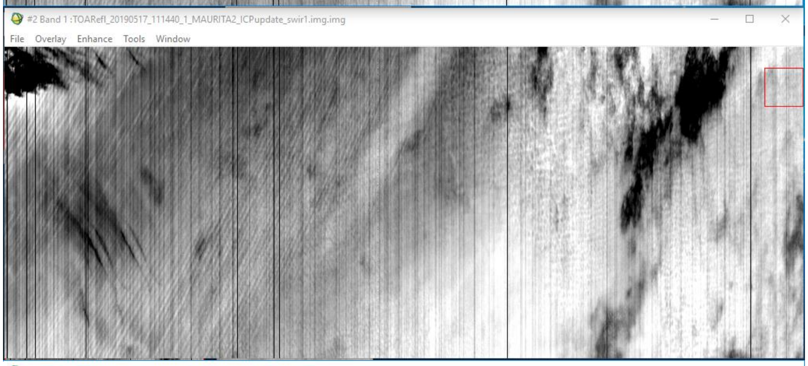

(Update LF + HF equalisation)

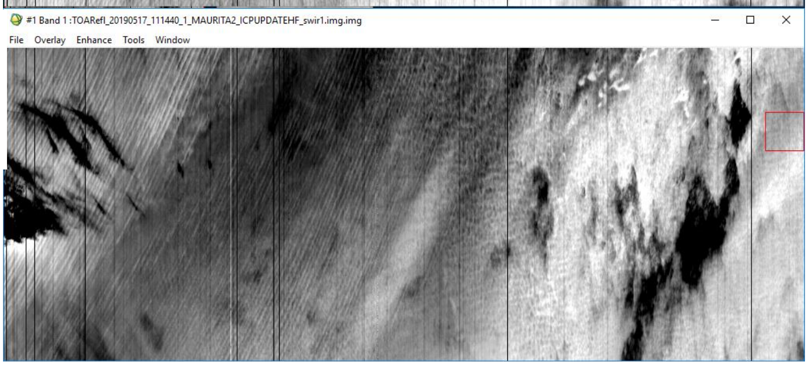

Figure 18. Visual assessments of the improvement of the scene uniformity through application of the yaw retrieved updates to the equalisation coefficients. (Note :black vertical lines are known BAD pixels). Results for LEFT SWIR1.

1.4.1.1. LEFT SWIR2

(Update to LF equalisation)

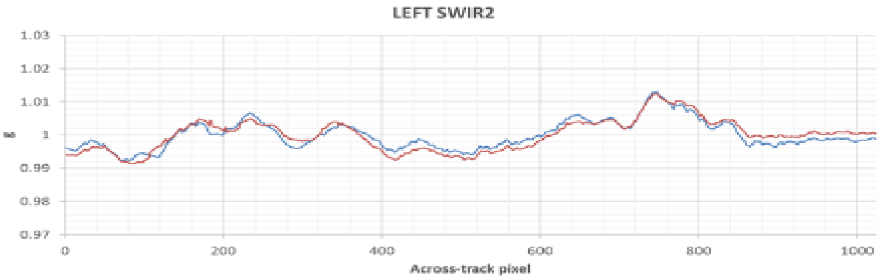

(Old)

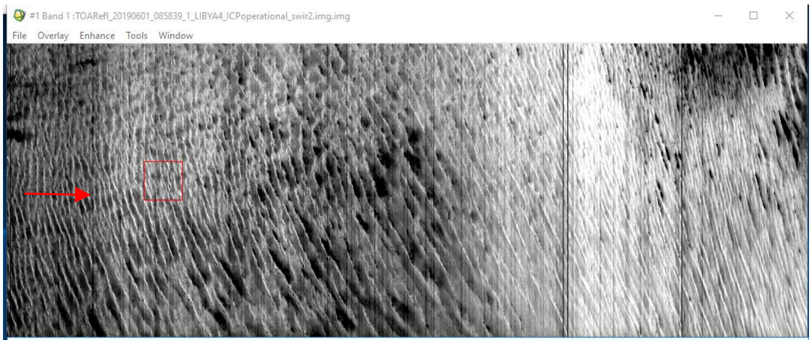

(Update LF equalisation)

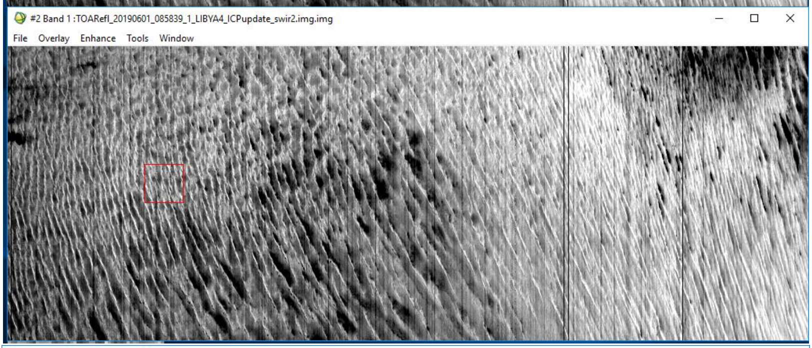

(Update LF + HF equalisation)

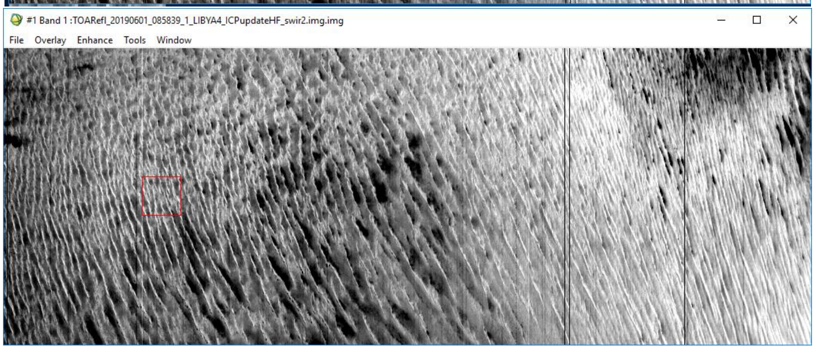

Figure 19. Visual assessments of the improvement of the scene uniformity through application of the yaw retrieved updates to the equalisation coefficients. (Note :black vertical lines are known BAD pixels). Results for LEFT SWIR2.

1.4.1.2. LEFT SWIR3

(Update to LF equalisation)

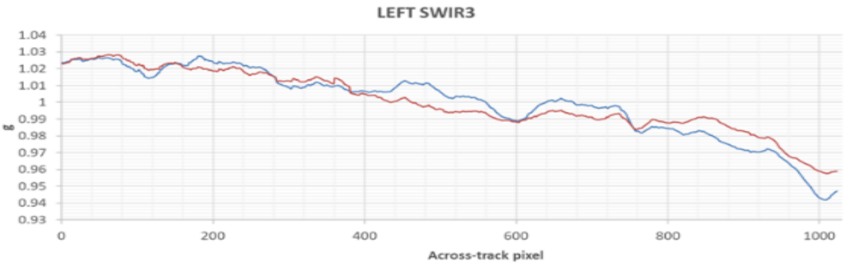

(Old)

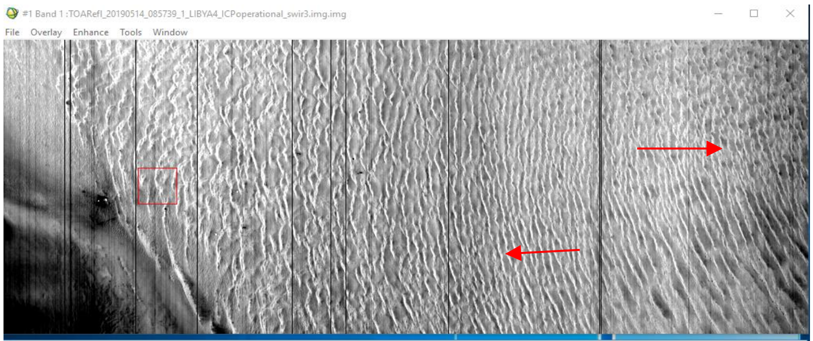

(Update LF equalisation)

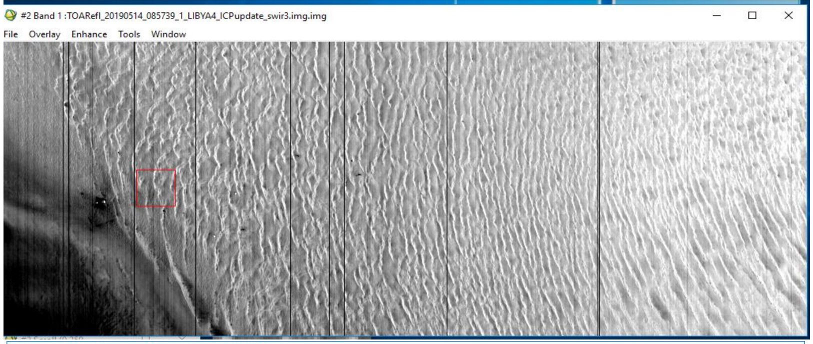

(Update LF + HF equalisation)

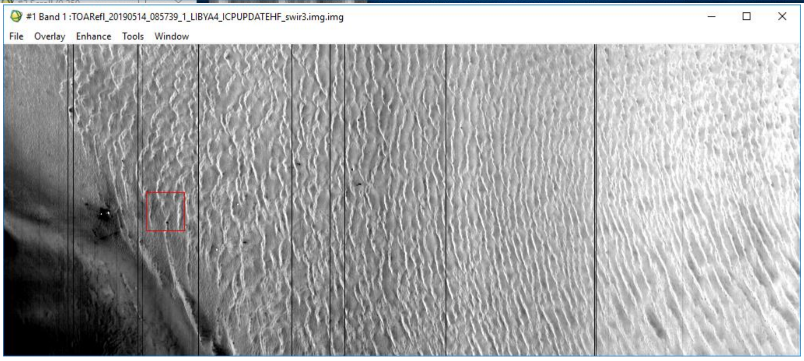

Figure 20. Visual assessments of the improvement of the scene uniformity through application of the yaw retrieved updates to the equalisation coefficients. (Note :black vertical lines are known BAD pixels). Results for LEFT SWIR3.

1.4.1. Right Camera

1.4.1.1. RIGHT SWIR1

(Update to LF equalisation)

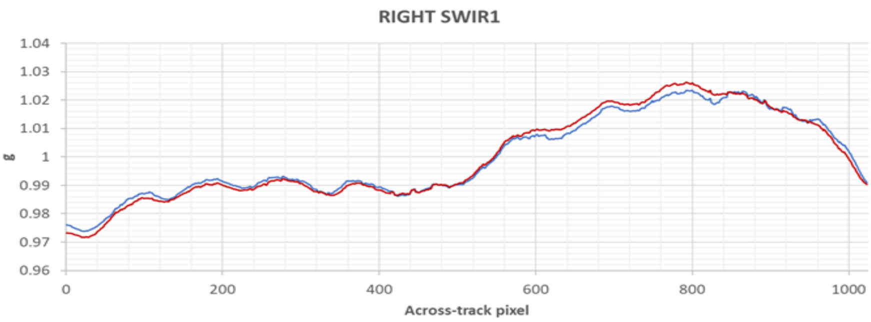

(Old)

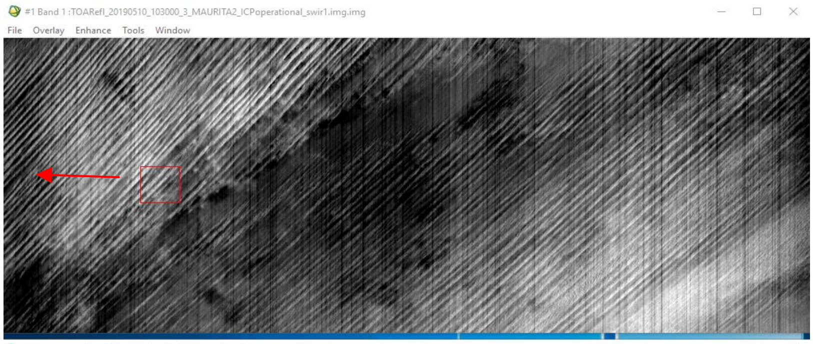

(Update LF equalisation)

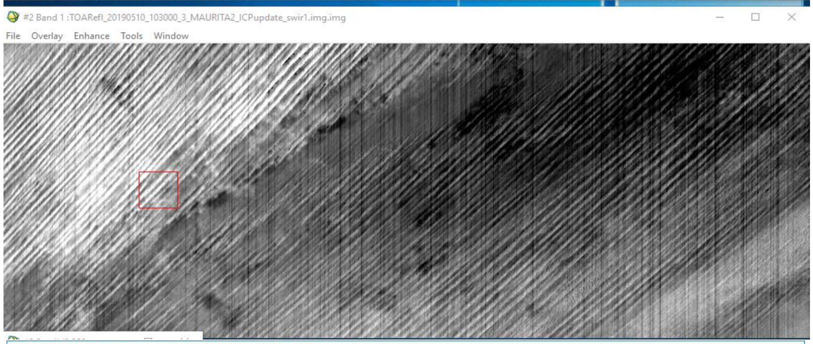

(Update LF + HF equalisation)

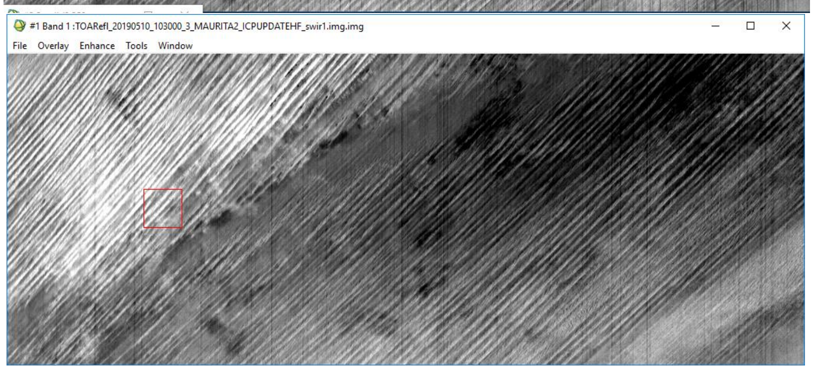

Figure 21. Visual assessments of the improvement of the scene uniformity through application of the yaw retrieved updates to the equalisation coefficients. (Note :black vertical lines are known BAD pixels). Results for RIGHT SWIR1.

1.4.1.2. RIGHT SWIR2

(Update to LF equalisation)

(Old)

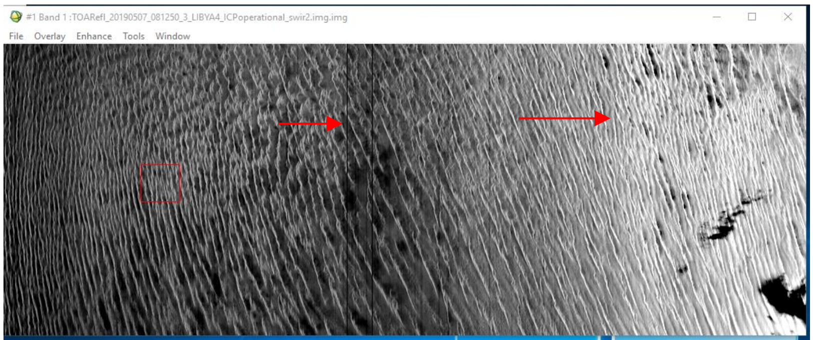

(Update LF equalisation)

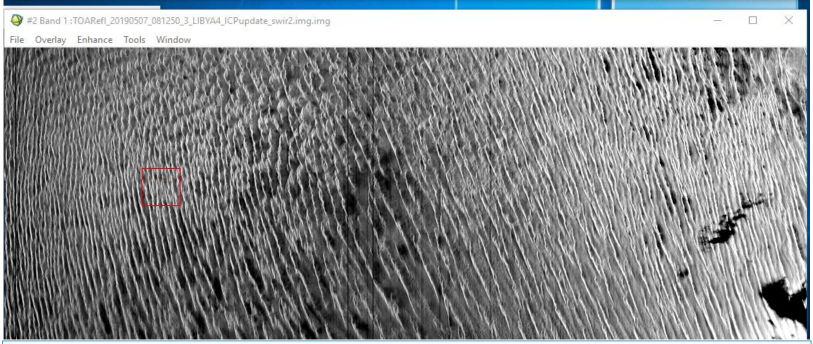

(Update LF + HF equalisation)

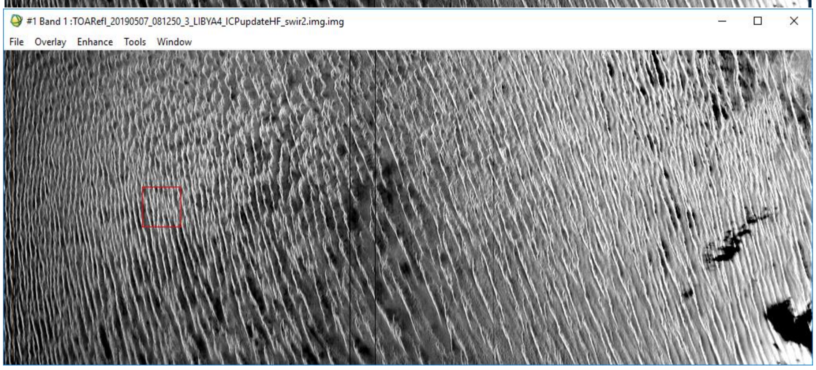

Figure 22. Visual assessments of the improvement of the scene uniformity through application of the yaw retrieved updates to the equalisation coefficients. (Note :black vertical lines are known BAD pixels). Results for RIGHT SWIR2.

1.4.1.3. RIGHT SWIR3

(Update to LF equalisation)

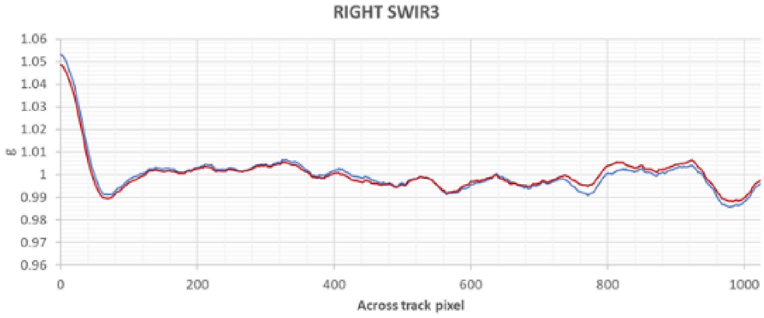

(Old)

(Update LF equalisation)

(Update LF + HF equalisation)

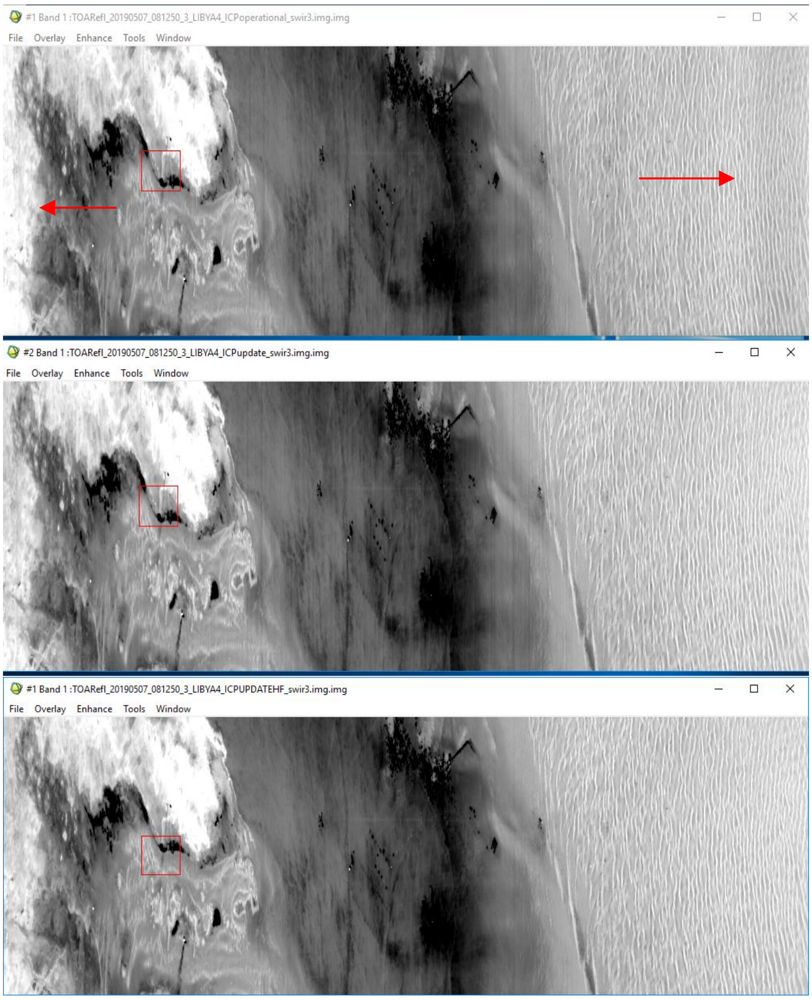

Figure 23. Visual assessments of the improvement of the scene uniformity through application of the yaw retrieved updates to the equalisation coefficients. (Note :black vertical lines are known BAD pixels). Results for RIGHT SWIR3.

1.5. Bad pixels

There are three new bad pixels identified in this reporting period.

Reporting period Mid-Mar 2019 - Mid June 2019																	
CAMERA	STRIP	pixel numbers (ID L1 A)															
		NEW BAD	BAD (from previous periods)														
left	swir1		3	28	39	104	298	345	352	644	956						
left	swir2	717	711	863													
left	swir3	82	90	172	250	370	419	438	568	759	761						
center	swir1	448	819	1021													
center	swir2		57	295	769	831	900										
center	swir3		29	30	99	131	448	476	579	640	763	804	889	890	917	938	994
right	swir1																
right	swir2		14	438	470												
right	swir3																

Table 6: Overview Bad pixels

1.6. Radiometric ICP file

The updates to the radiometric ICP file used within the user segment for the processing of the nominal PROBA-V data by PF are listed in the Table 9 for collection 1.

PROBAV_X_R_000_YEARMN01_**101**.xml*	Update dark currents Update of SWIR absolute following linear degradation model**
PROBAV_X_R_000_20161201_01.xml	Update dark currents Update of SWIR absolute following linear degradation model**
PROBAV_X_R_000_20161201_01.xml	Update dark currents Update of SWIR absolute following linear degradation model**
PROBAV_X_R_000_20161201_01.xml	Update dark currents Update of SWIR absolute following linear degradation model**
PROBAV_X_R_000_20161201_01.xml	Update dark currents Update of SWIR absolute following linear degradation model**
PROBAV_X_R_000_20170101_01.xml	Update dark currents Update of SWIR absolute following linear degradation model**
PROBAV_X_R_000_20170120_01.xml	SWIR status map updated : 1 bad pixel added
PROBAV_X_R_000_20170201_01.xml	Update dark currents Update of SWIR absolute following linear degradation model**
PROBAV_X_R_000_20170220_01.xml	SWIR status map updated : 1 bad pixel added

PROBAV_X_R_000_20170301_01.xml	Update dark currents Update of SWIR absolute following linear degradation model**
PROBAV_X_R_000_20170401_01.xml	Update dark currents Update of SWIR absolute following linear degradation model** SWIR status map updated : 1 bad pixel added
PROBAV_X_R_000_2017051_01.xml	Update dark currents Update of SWIR absolute following linear degradation model** Update of LEFT BLUE and CENTER BLUE absolute calibration coefficients following linear degradation model***
PROBAV_X_R_000_20170601_01.xml	Update dark currents Update of SWIR absolute following linear degradation model** Update of LEFT BLUE and CENTER BLUE absolute calibration coefficients following linear degradation model***
PROBAV_X_R_000_20170701_01.xml	Update dark currents Update of SWIR absolute following linear degradation model** Update of LEFT BLUE and CENTER BLUE absolute calibration coefficients following linear degradation model*** SWIR status map updated : 1 bad pixel added
PROBAV_X_R_000_20170801_01.xml	Update dark currents Update of SWIR absolute following linear degradation model** Update of LEFT BLUE and CENTER BLUE absolute calibration coefficients following linear degradation model*** SWIR status map updated : 2 bad pixel added
PROBAV_X_R_000_20170901_01.xml	Update dark currents Update of SWIR absolute following linear degradation model***, new coef applied for RIGHT SWIR strips***** Update of LEFT BLUE and CENTER BLUE absolute calibration coefficients following linear degradation model **with new coef** **** SWIR status map updated : 2 bad pixel added

PROBAV_X_R_000_20171001_01.xml	Update dark currents Update of SWIR absolute following linear degradation model***, new coef applied for RIGHT SWIR strips***** Update of LEFT BLUE and CENTER BLUE absolute calibration coefficients following linear degradation model **with new coef** ****
PROBAV_X_R_000_20171101_01.xml	Update dark currents Update of SWIR absolute following linear degradation model***, new coef applied for RIGHT SWIR strips***** Update of LEFT BLUE and CENTER BLUE absolute calibration coefficients following linear degradation model **with new coef** ****
PROBAV_X_R_000_20171201_01.xml	Update dark currents Update of SWIR absolute following linear degradation model***, new coef applied for RIGHT SWIR strips***** Update of LEFT BLUE and CENTER BLUE absolute calibration coefficients following linear degradation model **with new coef** ****
PROBAV_X_R_000_20180101_01.xml	Update dark currents Update of LEFT and CENTER SWIR absolute following linear degradation model***; **No update of RIGHT SWIR absolute cal**.. Update of LEFT BLUE and CENTER BLUE absolute calibration coefficients following linear degradation model **with new coef** ****
PROBAV_X_R_000_20180201_01.xml	Update dark currents Update of LEFT and CENTER SWIR absolute following linear degradation model***; **No update of RIGHT SWIR absolute cal**.. Update of LEFT BLUE and CENTER BLUE absolute calibration coefficients following linear degradation model **with new coef** ****
PROBAV_X_R_000_20180301_01.xml	Update dark currents Update of LEFT and CENTER SWIR absolute following linear degradation model***; **No update of RIGHT SWIR absolute cal**.. Update of LEFT BLUE and CENTER BLUE absolute calibration coefficients

	following linear degradation model **with new coef** ****
PROBAV_X_R_000_20180401_01.xml	Update dark currents Update of LEFT and CENTER SWIR absolute following linear degradation model***; **No update of RIGHT SWIR absolute cal**.. Update of LEFT BLUE and CENTER BLUE absolute calibration coefficients following linear degradation model **with new coef** ****
PROBAV_X_R_000_20180501_01.xml	Update dark currents Update of LEFT and CENTER SWIR absolute following linear degradation model***; **No update of RIGHT SWIR absolute cal**.. Update of LEFT BLUE and CENTER BLUE absolute calibration coefficients following linear degradation model **with new coef** ****
PROBAV_X_R_000_20180601_01.xml	Update dark currents Update of LEFT and CENTER SWIR absolute following linear degradation model***; **No update of RIGHT SWIR absolute cal**.. Update of LEFT BLUE and CENTER BLUE absolute calibration coefficients following linear degradation model **with new coef** ****
PROBAV_X_R_000_20180701_01.xml	Update dark currents Update of LEFT and CENTER SWIR absolute following linear degradation model***; **No update of RIGHT SWIR absolute cal**.. Update of LEFT BLUE and CENTER BLUE absolute calibration coefficients following linear degradation model **with new coef** ****
PROBAV_X_R_000_20180801_01.xml	Update dark currents Update of LEFT and CENTER SWIR absolute following linear degradation model***; **No update of RIGHT SWIR absolute cal**.. Update of LEFT BLUE and CENTER BLUE absolute calibration coefficients following linear degradation model **with new coef** ****

PROBAV_X_R_000_20180821_01.xml	SWIR status map updated : 1 bad pixel added for SWIR2 center camera + correction for assignment of bad pixel status to wrong pixel ID
PROBAV_X_R_000_20180901_01.xml	Update dark currents Update of LEFT and CENTER SWIR absolute following linear degradation model***; **No update of RIGHT SWIR absolute cal**.. Update of LEFT BLUE and CENTER BLUE absolute calibration coefficients following linear degradation model **with new coef** ****
PROBAV_X_R_000_20181001_01.xml	Update dark currents. Update of LEFT BLUE and CENTER BLUE absolute calibration coefficients following linear degradation model **with new coef** ****
PROBAV_X_R_000_20181101_01.xml	Update dark currents. Update of LEFT BLUE and CENTER BLUE absolute calibration coefficients following linear degradation model **with new coef** ****
PROBAV_X_R_000_20181201_01.xml	Update dark currents. Update of LEFT BLUE and CENTER BLUE absolute calibration coefficients following linear degradation model **with new coef** ****
PROBAV_X_R_000_20190101_01.xml	Update dark currents. Update of LEFT BLUE and CENTER BLUE absolute calibration coefficients following linear degradation model **with new coef** ****
PROBAV_X_R_000_2010201_01.xml	Update dark currents. Update of LEFT BLUE and CENTER BLUE absolute calibration coefficients following linear degradation model **with new coef** ****

PROBAV_X_R_000_20190301_01.xml	Update dark currents. Update of LEFT BLUE and CENTER BLUE absolute calibration coefficients following linear degradation model **with new coef** ****
PROBAV_X_R_000_20190401_01.xml	Update dark currents. Update of LEFT BLUE and CENTER BLUE absolute calibration coefficients following linear degradation model **with new coef** ****
PROBAV_X_R_000_20190501_01.xml	Update dark currents. Update of LEFT BLUE and CENTER BLUE absolute calibration coefficients following linear degradation model **with new coef** **** One new bad pixel added : left SWIR3 PixelID 82 (0-based)
PROBAV_X_R_000_20190601_01.xml	Update dark currents. Update of LEFT BLUE and CENTER BLUE absolute calibration coefficients following linear degradation model **with new coef** **** Two new bad pixel added : left SWIR2 PixelID 717 (0-based) and CENTER SWIR1 PixelID 448
PROBAV_X_R_000_20190701_01.xml	Update dark currents. Update of LEFT BLUE and CENTER BLUE absolute calibration coefficients following linear degradation model **with new coef** **** Update equalization coefficients LEFT and RIGHT SWIR strips based on Yaw maneuver analyses.

Table 7: Radiometric ICP-file updates Collection 1

2. Geometric Image Quality

2.1. Summary

The quarterly Average Location Error (ALE) over the period 16/3/2018 – 15/6/2019 was 67 m (1б = 84 m) for all spectral bands (combined cameras). Compared to the previous reporting period, the ALE has decreased (improved) by 10%. The total number of ground control points used was 427,158, which is 79% higher than in previous quarter.

The daily average location error compliance (ALE < 300m) was 99.24%, which is 0.01% higher than in previous quarter. The inter-band geometric accuracy was 33 – 54 m (standard deviation range is 8 – 16 m), which is 0.10 – 0.16 of a pixel (333 m). The average inter-band RED-NIR registration accuracy was 33 m, which is 1 m lower than in previous reporting period.

The multi-temporal geometric accuracy was 84.64% (3.66% higher compared to previous quarter) for the VNIR and 94.94% (0.32% higher compared to previous quarter) for the combined VNIR/SWIR. The multi-temporal accuracies over the last full year are 72.32% and 87.91% for VNIR and VNIR/SWIR, respectively.

The geometric ICP file generated on 8/9/2016, valid from 1/9/2016 has remained valid throughout the reporting period.

2.2. Assessment of the geometric accuracy on L1C data

The absolute location error (ALE) and accompanying standard deviation of the Level1C data is presented in the tables below for each camera, spectral band/strip and reporting month.

CAMERA 1 Mean and standard deviation ALE [m]			
Strip\Period	**16/3/2019 - 15/4/2019**	**16/4/2019 - 15/5/2019**	**16/5/2019 - 15/6/2019**
BLUE	54.55, σ = 31.10	54.28, σ = 31.40	57.01, σ = 33.53
RED	55.27, σ = 32.08	55.94, σ = 33.22	58.65, σ = 35.45
NIR	57.42, σ = 33.56	57.01, σ = 33.18	58.00, σ = 33.91
SWIR1	82.29, σ = 50.86	82.82, σ = 51.50	84.80, σ = 53.51
SWIR2	57.46, σ = 31.37	57.25, σ = 31.01	58.84, σ = 32.63
SWIR3	52.59, σ = 29.14	52.75, σ = 28.97	57.01, σ = 31.63

Table 8: Mean absolute location error and standard deviation (σ) for camera 1.

CAMERA 2 Mean and standard deviation ALE [m]			
Strip\Period	**16/3/2019 - 15/4/2019**	**16/4/2019 - 15/5/2019**	**16/5/2019 - 15/6/2019**
BLUE	63.16, σ = 36.00	67.17, σ = 35.43	74.46, σ = 37.67
RED	64.97, σ = 37.02	70.93, σ = 37.36	76.55, σ = 37.96
NIR	62.11, σ = 35.59	67.68, σ = 35.96	73.32, σ = 36.79
SWIR1	65.97, σ = 38.06	70.16, σ = 37.25	72.98, σ = 37.13
SWIR2	65.00, σ = 37.92	69.73, σ = 37.64	73.45, σ = 37.95
SWIR3	63.43, σ = 37.64	67.61, σ = 37.44	72.08, σ = 38.57

Table 9: Mean absolute location error and standard deviation (σ) for camera 2.

CAMERA 3 Mean and standard deviation ALE [m]			
Strip\Period	**16/3/2019 - 15/4/2019**	**16/4/2019 - 15/5/2019**	**16/5/2019 - 15/6/2019**
BLUE	65.17, σ = 35.58	58.81, σ = 35.08	58.61, σ = 32.62
RED	69.82, σ = 39.19	61.20, σ = 38.27	58.77, σ = 34.53
NIR	66.05, σ = 39.40	58.13, σ = 36.81	55.26, σ = 32.74
SWIR1	60.16, σ = 34.03	54.88, σ = 32.73	54.54, σ = 30.88
SWIR2	68.57, σ = 38.80	60.84, σ = 36.47	59.27, σ = 33.66
SWIR3	90.98, σ = 54.47	81.17, σ = 51.08	78.32, σ = 47.60

Table 10: Mean absolute location error and standard deviation (σ) for camera 3.

In the reporting period the average location error of the Level 1C data was 65 m, which is 5 m (7%) lower than in the previous quarter.

2.3. Assessment of the geometric accuracy on L2 data

2.3.1. Absolute geometric accuracy

The daily summary of the L2 data absolute location error for all spectral bands is presented in the tables and figures below for the three reporting months:

- from 16/3/2019 – 15/4/2019
- from 16/4/2019 – 15/5/2019
- from 16/5/2019 – 15/6/2019

The tables list:

- The day of the measurement in format dd-mm-yy
- The daily achieved compliance (%B) for the BLUE band (% of GCP where ALE <=300m)
- The daily achieved compliance (%R) for the RED band (% of GCP where ALE <=300m)
- The daily achieved compliance (%N) for the NIR band (% of GCP where ALE <=300m)
- The daily achieved compliance (%S) for the SWIR band (% of GCP where ALE <=450m)

- The number of GCP per day (NB-B) used to derive the absolute location error ALE for the BLUE band
- The daily average ALE (in m) for the BLUE band (MU-B)
- The daily ALE standard deviation (in m) for the BLUE band (STD-B)

- The number of GCP per day (NB-R) used to derive the absolute location error ALE for the RED band
- The daily average ALE (in m) for the RED band (MU-R)
- The daily ALE standard deviation (in m) for the RED band (STD-R)

- The number of GCP per day (NB-N) used to derive the absolute location error ALE for the NIR band
- The daily average ALE (in m) for the NIR band (MU-N)
- The daily ALE standard deviation (in m) for the NIR band (STD-N)

- The number of GCP per day (NB-S) used to derive the absolute location error ALE for the SWIR band
- The daily average ALE (in m) for the SWIR band (MU-S)
- The daily ALE standard deviation (in m) for the SWIR band (STD-S)

Day	%B	%R	%N	%S	NB-B	MU-B	STD-B	NB-R	MU-R	STD-R	NB-N	MU-N	STD-N	NB-S	MU-S	STD-S
16/03/2019	98.56	99.18	99.26	99.66	28491	76.26	101.28	32452	70.36	88.36	32828	67.97	84.35	32159	70.17	85.91
17/03/2019	98.66	99.35	99.28	99.72	31737	71.08	98.73	35214	63.38	78.76	34462	61.88	76.06	32942	65.06	81.45
18/03/2019	98.99	99.32	99.4	99.77	27605	65.9	87.46	32711	61.17	80.96	31931	59.2	72.8	31570	61.33	71.27
19/03/2019	98.85	99.34	99.44	99.68	24780	67.5	97.63	30142	60.57	92.72	29762	58.14	73.98	30842	62.91	86.96
20/03/2019	98.88	99.4	99.35	99.67	27267	68.99	89.08	30598	63.6	78.95	31120	61.65	77.93	31443	65.29	85.13
21/03/2019	98.76	99.38	99.35	99.67	28228	72.61	98.8	31541	64.62	80.37	30550	63.76	80.41	30768	65.82	81.69
22/03/2019	98.9	99.45	99.4	99.7	23872	70.55	93.79	28457	62.35	77.49	27486	62.58	80.57	27312	66.41	91.55
23/03/2019	98.76	99.19	99.11	99.71	19158	86.63	96.73	23883	78.41	81.37	23367	76.43	81.61	26493	77.62	87.82
24/03/2019	98.58	98.99	99.06	99.73	19750	86.59	101.32	25038	80.89	91.64	25240	77.26	86.14	28025	77.53	74.04
25/03/2019	98.58	99.19	99.3	99.71	22382	87.08	104.48	27010	78.96	81.67	26968	75.22	78.91	28341	77.04	84.03
26/03/2019	98.8	99.33	99.41	99.69	22429	77.04	93.55	26685	69.19	84.03	26945	65.5	74.06	26303	68.6	79.43
27/03/2019	98.99	99.44	99.29	99.69	21508	70.03	92.66	24059	62.13	72.96	25155	62.31	77.72	23558	65.37	78.45
28/03/2019	98.91	99.45	99.54	99.76	23464	69.93	97.42	28536	61.98	77.41	28342	59	74.46	28672	62.93	76.25
29/03/2019	98.65	99.26	99.23	99.66	25784	68.39	97.5	29771	62.04	85.49	29280	62.81	90.55	30346	63.82	84.22
30/03/2019	98.55	99.21	99.25	99.58	24450	71.77	109.28	28505	62.23	89.85	27879	63.29	95.34	28853	65.18	94.83
31/03/2019	98.82	99.25	99.24	99.69	26182	70.3	94.39	31384	62.83	75.86	30602	62.56	75.44	31521	66.53	83.05
01/04/2019	98.99	99.39	99.35	99.68	44736	69.05	93.11	42194	61.79	82.52	35580	60.54	72.18	34925	65.44	89.92
02/04/2019	98.82	99.29	99.41	99.76	26770	72.51	92.04	31132	66.8	75.78	32143	64.61	72.57	33729	68.39	73.86
03/04/2019	98.73	99.27	99.29	99.7	30711	75.3	88.92	32317	69.13	70.32	31920	67.52	76.49	32903	70.95	84.61
04/04/2019	98.55	99.04	98.89	99.64	26486	85.63	100.22	30218	79.56	86.81	29326	76.19	79.88	29548	79.66	85.12
05/04/2019	98.56	98.99	99.08	99.67	23980	83.94	95.36	27702	78.78	86.76	28456	74.84	81.54	27420	77.17	83.1
06/04/2019	98.61	99.27	99.24	99.65	23661	74.25	99.29	28633	66.63	75.01	29298	65.99	87.45	28834	69.44	90.7
07/04/2019	98.6	99.18	99.27	99.7	28791	71.63	97.27	32363	66.81	86.17	31508	65.23	83.49	32291	67.76	81.22
08/04/2019	98.65	99.27	99.29	99.64	34597	76.08	94.4	37339	70.12	79.76	35694	68.53	81.25	33984	69.85	80.43
09/04/2019	98.66	99.25	99.3	99.69	31954	73.93	95.58	36676	66.47	79.64	36102	64.77	77.51	35132	66.53	79.66
10/04/2019	98.94	99.35	99.35	99.7	30328	66.77	88.66	34972	60.15	65.47	35260	59.44	71.08	33872	63.09	82.47
11/04/2019	98.81	99.17	99.23	99.71	27783	69.47	93.6	32107	65.82	82.95	32729	62.47	79.93	32425	65.87	79.45
12/04/2019	98.44	99.13	99.08	99.57	26743	83.47	105.42	29642	78.08	83.69	29687	74.28	84.69	29139	78.37	88.8
13/04/2019	98.24	99.07	99.14	99.58	26836	82.95	101.3	29741	77.12	80.22	28129	72.62	85.75	27553	76.48	84.24
14/04/2019	98.75	99.06	99.08	99.71	26166	72.24	87.58	30672	67.39	86.06	29807	63.68	87.16	30837	65.59	85.8
15/04/2019	99.01	99.46	99.1	99.51	9906	71.36	91.75	10963	61.44	66.81	10106	65.62	79.29	11722	66.9	95.97
Averages	**98.73**	**99.26**	**99.26**	**99.68**	**26339**	**74.49**	**96.08**	**30085**	**67.77**	**80.83**	**29602**	**66.0**	**80.02**	**29789**	**68.81**	**83.59**

Table 11: Daily achieved compliance and the daily average location error (in m) for all spectral bands in the period 16/3/2019 – 15/4/2019.

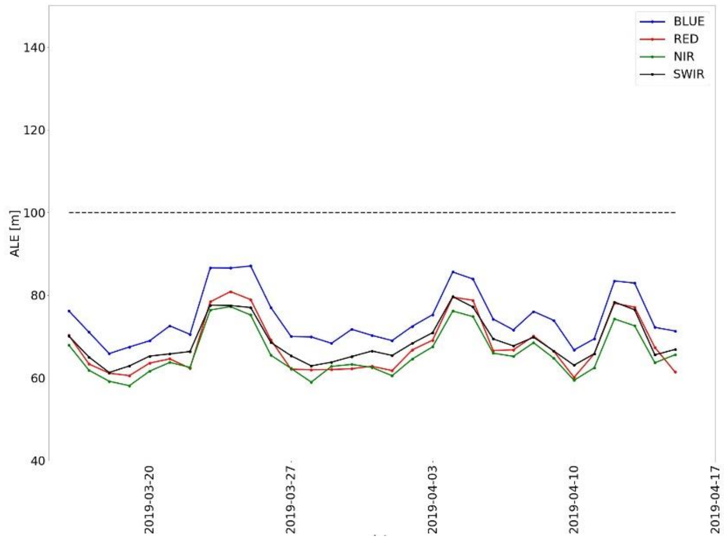

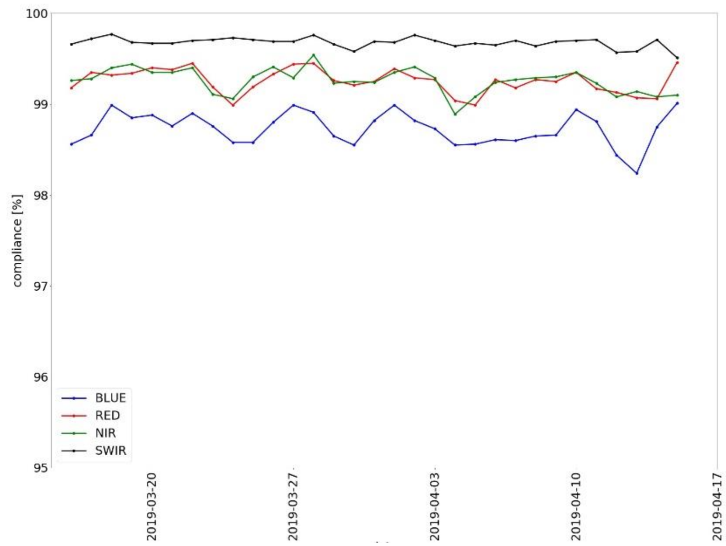

Figure 24: Daily average location error in the period from 16/3/2019 – 15/4/2019 (left) and the average daily compliance of the spectral bands (right).

Day	%B	%R	%N	%S	NB-B	MU-B	STD-B	NB-R	MU-R	STD-R	NB-N	MU-N	STD-N	NB-S	MU-S	STD-S
16/04/2019	98.77	99.24	99.23	99.67	26082	66.81	96.11	30484	60.96	85.83	31250	59.31	85.69	32955	61.22	74.95
17/04/2019	98.66	99.2	99.23	99.6	32258	66.4	91.19	37180	58.88	83.56	37341	58.77	82.92	37484	61.55	84.9
18/04/2019	98.78	99.26	99.21	99.73	34034	65.07	98.48	38778	57.62	77.68	38022	58.19	80.81	37681	60.69	68.84
19/04/2019	99.1	99.39	99.43	99.73	33501	62.58	85.06	38276	56.08	77.07	37514	56.44	75.35	39440	57.69	72.78
20/04/2019	98.79	99.3	99.4	99.71	30564	67.27	91.74	34538	61.55	80.67	35569	62.62	79.47	35256	63.95	76.85
21/04/2019	98.51	99.17	99.24	99.71	31247	68.08	96	35760	60.6	81.11	36355	61.57	83.17	37081	62.56	79.79
22/04/2019	98.91	99.41	99.32	99.68	30942	65.4	92.46	35206	58.18	78.04	35929	59.24	82.04	34539	61.31	81.67
23/04/2019	98.8	99.22	99.24	99.72	30262	67.31	91.49	34873	60.12	76.43	34549	57.69	75.12	34368	59.82	78.92
24/04/2019	98.82	99.33	99.39	99.71	29589	74.23	98.28	34885	67.54	80.54	34660	63.23	79.33	36727	67.1	82.36
25/04/2019	98.79	99.19	99.21	99.71	32091	69.07	97.4	36943	64.48	89.19	36357	61.5	78.73	39072	64.6	78.82
26/04/2019	98.59	99.14	99.18	99.59	31910	71.29	98.71	35676	64.45	81.13	34940	62.85	85.77	36216	66.23	92.23
27/04/2019	98.92	99.27	99.18	99.73	36189	69.48	93.05	41154	63.75	78.39	39431	62.92	87.24	40415	64.44	72.81
28/04/2019	98.98	99.22	99.22	99.71	32153	63.03	95.26	36816	58.28	77.04	37441	56.77	77.88	37692	59.01	78.11
29/04/2019	98.8	99.3	99.26	99.69	30988	68.37	98.76	37073	63.12	84.34	37806	61.68	84.92	39325	63.45	79.35
30/04/2019	98.44	98.91	98.98	99.64	30144	80.06	98.65	34409	77.38	88.03	34065	75.53	86.27	34514	75.82	87.98
01/05/2019	98.38	98.87	98.87	99.64	31810	90.34	102.82	35407	86.75	92.62	33669	84.71	86.62	35344	83.38	82.51
02/05/2019	98.84	99.23	99.14	99.69	30658	78.6	94.07	34509	74.1	86.9	33740	70.91	79.19	33467	74.33	81.86
03/05/2019	99.1	99.43	99.38	99.74	35064	72.62	97.31	40124	67.18	76.31	38734	65.7	81.77	39597	67.57	72.3
04/05/2019	98.74	99.24	99.31	99.71	32615	68.01	98.71	37532	62.34	78.6	36546	61.56	77.59	38689	63.24	75.86
05/05/2019	98.8	99.28	99.32	99.66	36033	69.19	102.79	40500	61.92	76.73	39161	61.48	79.04	40979	63.74	80.08
06/05/2019	98.68	99.14	99.2	99.71	38258	70.82	96.42	43028	65.03	79.8	40875	62.64	81.52	42405	63.65	77.01
07/05/2019	98.78	99.07	99.23	99.7	36149	70.58	87.42	41382	64.45	77.22	39953	63.06	73.51	41969	63.09	76.17
08/05/2019	98.81	99.31	99.3	99.74	33885	66.9	88.22	39877	60.12	80.61	38256	59.01	78.53	40535	61.1	74.45
09/05/2019	98.56	99.19	99.27	99.68	32167	70.06	101.3	38532	62.78	80.5	38149	60.62	79.3	38905	63.51	78.87
10/05/2019	98.6	99.09	99.13	99.69	37810	72.13	97.75	44170	65.95	83.28	41180	64.92	81.13	42025	66.28	75.78

11/05/2019	98.77	99.18	99.16	99.74	37065	72.82	91.85	43716	67.17	75.15	42042	65.36	75.19	44080	67.33	79.84
12/05/2019	99	99.3	99.27	99.74	37828	69.02	87.43	44285	63.06	77.79	43575	61.69	76.26	45121	65.45	80.47
13/05/2019	98.86	99.23	99.23	99.69	35501	68.43	96.21	41436	62.8	77.23	41937	61.42	80.66	42830	64.93	79.55
14/05/2019	98.75	99.12	99.18	99.62	35995	73.04	96.69	40186	68.8	85.56	40784	65.8	87.71	40436	69.29	88.45
15/05/2019	98.64	98.93	99	99.64	32177	80.2	91.87	38173	76.86	90.03	39037	71.29	80.85	38808	74.13	88.06
Averages	**98.77**	**99.21**	**99.22**	**99.69**	**33165**	**70.57**	**95.12**	**38163**	**64.74**	**81.25**	**37628**	**63.28**	**80.79**	**38598**	**65.35**	**79.39**

Table 12: Daily achieved compliance and the daily average location error (in m) for all spectral bands in the period 16/4/2019 – 15/5/2019.

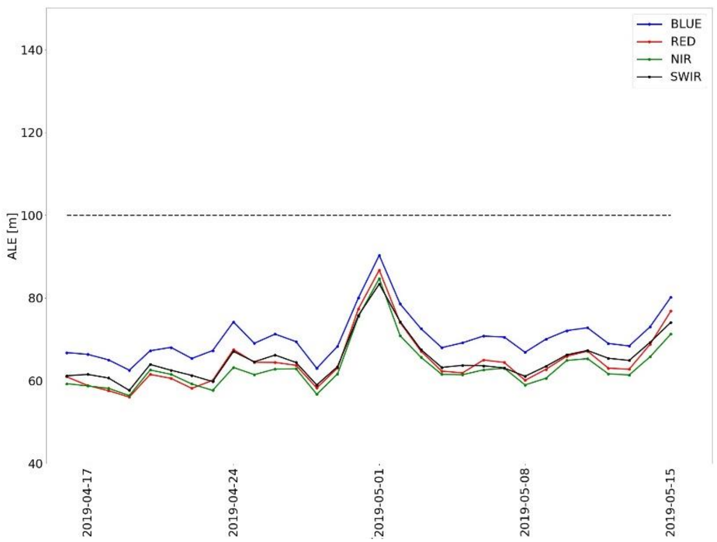

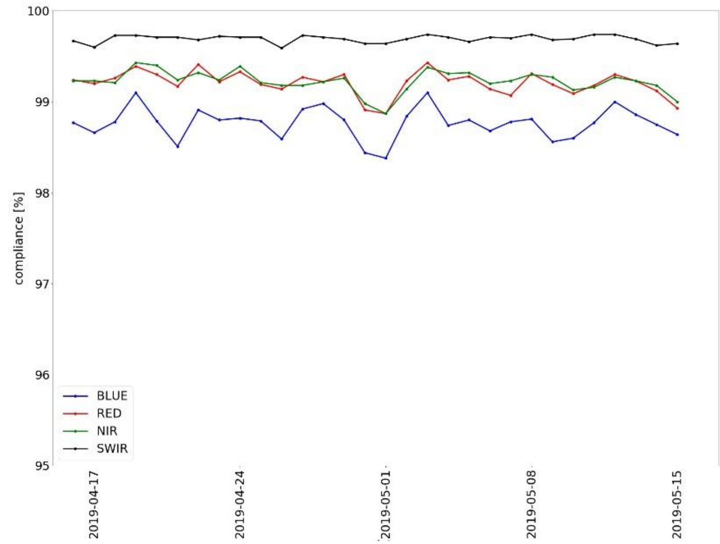

Figure 25: Daily average location error in the period from 16/4/2019 – 15/5/2019 (left) and the average daily compliance of all spectral bands (right).

Day	%B	%R	%N	%S	NB-B	MU-B	STD-B	NB-R	MU-R	STD-R	NB-N	MU-N	STD-N	NB-S	MU-S	STD-S
16/05/2019	98.79	98.94	98.97	99.68	31467	80.61	90.25	37647	76.66	83.4	39297	72.65	90.11	39765	72.74	86.89
17/05/2019	98.73	99.25	99.2	99.66	28631	74.1	94.59	34244	67.77	78.59	36077	65.14	93.29	37784	66.82	83.25
18/05/2019	98.82	99.36	99.44	99.74	29586	68.91	96.76	35406	61.33	74.32	37245	57.07	74.74	38239	62.07	79.63
19/05/2019	98.7	99.39	99.46	99.73	29994	69.42	92.43	37769	61.67	90.15	40223	56.51	76.53	41123	60.81	74.13
20/05/2019	98.81	99.31	99.44	99.68	29398	67.74	96.05	37736	58.91	85.68	38126	55.44	73.32	41370	59.27	80.21
21/05/2019	99.1	99.47	99.45	99.71	33281	62.98	93.02	41703	55	71.24	41823	54.8	69.95	44907	58.01	78.05
22/05/2019	98.64	99.19	99.34	99.75	29883	68.84	99.44	35963	62.43	88.05	37168	60.08	81.48	39006	62.12	78.22
23/05/2019	98.39	99.06	99.12	99.64	29619	78.67	99.13	34539	71.91	88.68	36042	70.72	88.89	35859	73.47	83.96
24/05/2019	98.54	99.16	99.26	99.62	29663	77.39	99.93	36536	69	88.15	37226	67.58	79.95	35322	72.29	83.1
25/05/2019	98.65	99.24	99.35	99.73	31843	72.43	94.66	38700	65.44	83.23	38873	65.23	69.15	39826	66.61	77.89
26/05/2019	98.88	99.46	99.5	99.73	32911	65.82	95.88	40184	56.67	70.08	42263	56.03	73.31	45199	58.52	78.35
27/05/2019	98.78	99.26	99.36	99.77	33770	65.08	92.72	41070	59.85	78.82	44954	58.54	82.01	46252	59.23	73.96
28/05/2019	98.64	99.23	99.35	99.79	35092	69	97.33	41956	63.51	79.73	42557	60.83	76.17	44378	62.95	71.03
29/05/2019	98.7	99.04	99.2	99.74	36680	74.5	101.58	43415	69.78	82.29	45728	65.71	71.96	46027	69.13	77.47
30/05/2019	99.02	99.3	99.34	99.71	35537	70.03	90.34	43685	64.4	73.25	44765	60.94	74.83	47106	63.29	79.35
31/05/2019	98.78	99.24	99.32	99.68	27096	70.24	103.94	33520	61.79	84.7	32812	58.92	82.58	33933	61.28	74.81
01/06/2019	98.82	99.22	99.33	99.67	31150	70.04	93.85	37650	64.33	85.97	39092	62.16	79.56	38087	64.75	80.64
02/06/2019	98.67	99.11	99.3	99.69	33934	75.3	101.52	40718	69.61	80.15	39908	66.63	77.97	39455	71.21	85.46
03/06/2019	98.86	99.1	99.13	99.73	34909	73.29	92.83	41788	68.79	82.22	42117	66.98	80.42	41650	68.74	72.89
04/06/2019	98.84	99.4	99.41	99.77	34050	70.2	99.24	41434	62.04	71.34	42733	61.29	71.78	43400	64.01	72.99
05/06/2019	98.86	99.29	99.36	99.7	35475	67.18	87.05	43757	61.67	80.03	45745	59.84	72.61	46592	63.73	77.24
06/06/2019	98.82	99.3	99.43	99.74	39670	67.34	91.76	48916	59.79	72.87	50719	57.43	71.49	50266	61.2	76.13
07/06/2019	98.78	99.22	99.36	99.74	38275	70.7	90.99	48494	63.64	75.48	52036	58.75	70.28	50882	62.79	76.44
08/06/2019	98.93	99.29	99.43	99.78	38253	73.65	88.95	48351	67.11	75.41	52617	61.43	73.42	53406	64.38	69.67
09/06/2019	99.11	99.5	99.55	99.78	36975	64.15	88.77	45661	57.54	74.65	50721	52.99	65.48	51421	56.62	69.54
10/06/2019	98.77	99.16	99.3	99.66	34737	67.55	99.94	42971	61.14	80.21	47180	56.79	78.38	46791	60.49	81.52
11/06/2019	98.67	99.24	99.35	99.73	37033	73.02	91.59	47016	66.39	76.31	49284	60.49	71.6	49771	64.77	81.49
12/06/2019	98.71	99.03	99.25	99.75	36309	74.04	95.08	45569	68.88	80.34	47767	63.51	71.03	48487	65.63	75.91
13/06/2019	98.96	99.39	99.46	99.76	38837	72.83	88.48	48278	67.1	72.28	52872	61.8	69.1	53118	64.92	74.92
14/06/2019	98.79	99.22	99.34	99.76	38947	70.81	103.5	47643	64.73	81.34	52521	59.98	74.52	52109	63.76	70.3
15/06/2019	98.78	99.16	99.31	99.71	41485	71.89	93.53	50814	64.82	79.92	54849	58.52	74.1	53048	63.5	73.61
Averages	**98.79**	**99.24**	**99.34**	**99.72**	**34015**	**70.9**	**95.0**	**41713**	**64.31**	**79.64**	**43720**	**61.12**	**76.13**	**44341**	**64.16**	**77.39**

Table 13: Daily achieved compliance and the daily average location error (in m) for all spectral bands in the period 16/5/2019 – 15/6/2019.

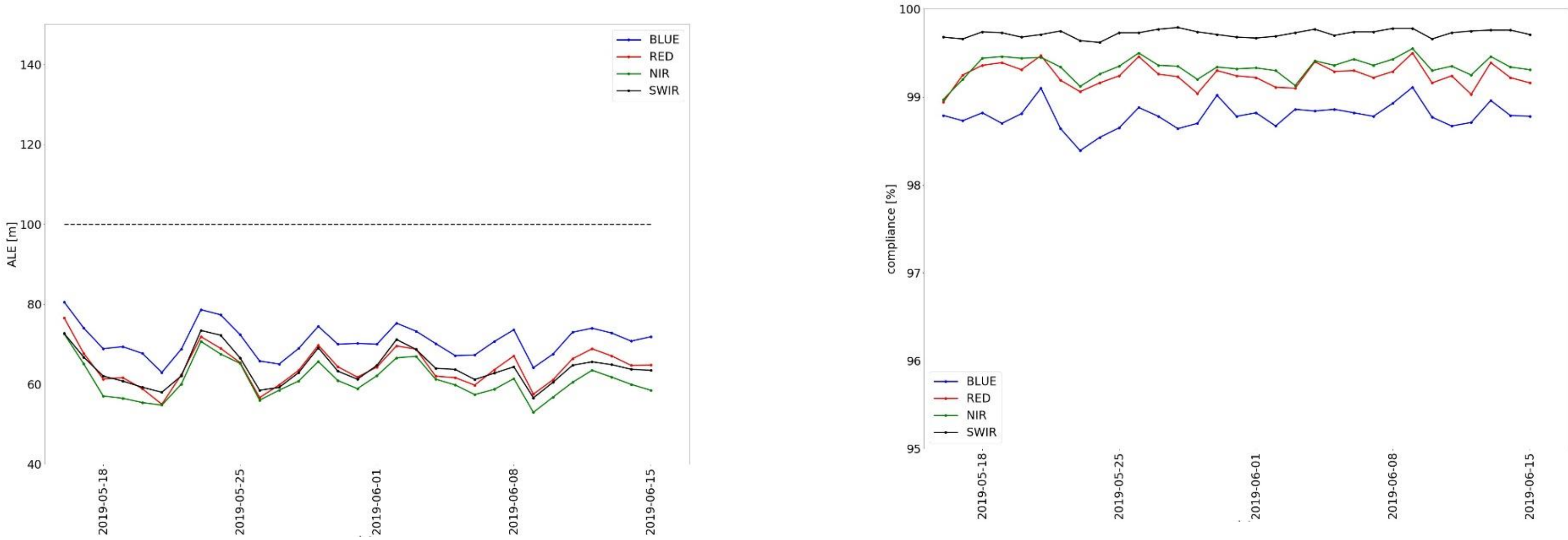

Figure 26: Daily average location error in the period from 16/5/2019 – 15/6/2019 (left) and the average daily compliance of all spectral bands (right).

2.3.2. Inter-band geometric accuracy

The monthly average inter-band geolocation error for all spectral band combinations was as follows:

Band pair	Inter-band error [m]
BLUE-RED	34.81, σ = 9.45
BLUE-NIR	50.30, σ = 15.89
BLUE-SWIR	53.60, σ = 13.57
RED-NIR	33.28, σ = 14.66
RED-SWIR	42.98, σ = 9.50
NIR-SWIR	43.19, σ = 8.08

Table 14: Inter-band geolocation accuracy and standard deviation for period 16/3/2018 – 15/4/2019 for the combined cameras, at 95% confidence level.

Band pair	Inter-band error [m]
BLUE-RED	33.69, σ = 9.32
BLUE-NIR	49.86, σ = 15.85
BLUE-SWIR	51.65, σ = 13.51
RED-NIR	33.77, σ = 14.44
RED-SWIR	41.04, σ = 9.50
NIR-SWIR	40.82, σ = 7.88

Table 15: Inter-band geolocation accuracy and standard deviation for period 16/4/2019 – 15/5/2019 for the combined cameras, at 95% confidence level.

Band pair	Inter-band error [m]
BLUE-RED	32.55, σ = 9.11
BLUE-NIR	48.36, σ = 13.87
BLUE-SWIR	49.97, σ = 12.35
RED-NIR	33.15, σ = 12.04
RED-SWIR	40.84, σ = 8.55
NIR-SWIR	39.73, σ = 7.23

Table 16: Inter-band geolocation accuracy and standard deviation for period 16/5/2019 – 15/6/2019 for the combined cameras, at 95% confidence level.

For the combined cameras, the inter-band geometric accuracy range was 33 – 54 m (standard deviation range is 8 – 16 m), which is 0.10 – 0.16 of a pixel (333 m). The average inter-band RED-NIR registration accuracy was 33 m, which is 1 m lower than previous reporting period.

2.3.3. Multi-temporal geometric accuracy

During this reporting period the multi-temporal compliance of the geometric accuracy was:

- 84.64% for the VNIR sensor (152,035 GCPs used),
- 94.94% for the VNIR/SWIR combined (193,272 GCPs used).

The multi-temporal geometric accuracy was 84.64% (3.66% higher compared to previous quarter) for the VNIR and 94.94% (0.32% higher compared to previous quarter) for the combined VNIR/SWIR. The multi-temporal accuracies over the last full year are 72.32% and 87.91% for VNIR and VNIR/SWIR, respectively.

For the VNIR the multi-temporal geometric accuracy is below the requirements. A map of regions with decreased multi-temporal geometric accuracy is presented in

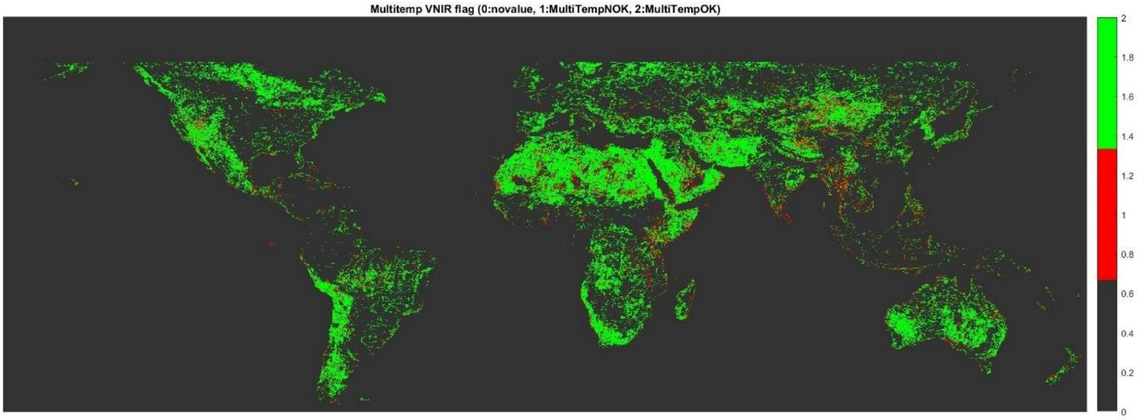

Figure 27.

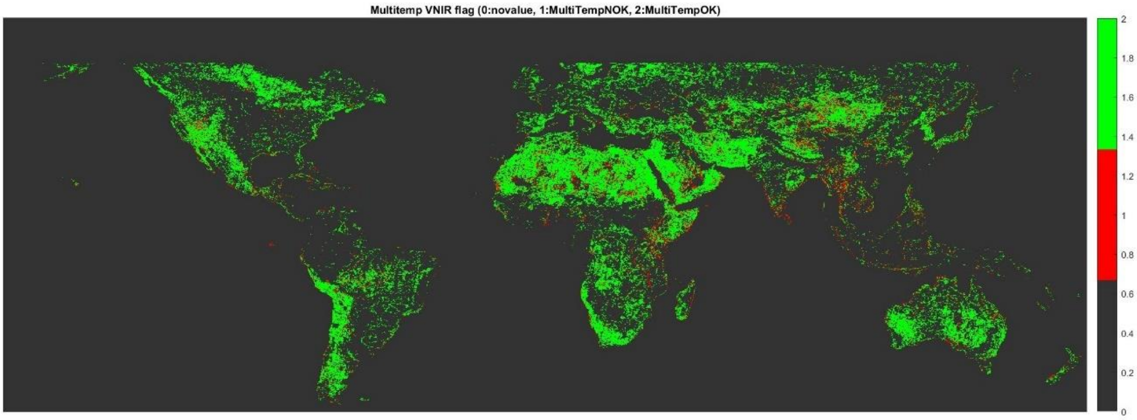

Figure 27: Multi-temporal geometric accuracy for the VNIR sensor for 16/3/2019 – 15/6/2019. Compliant areas are marked in green; areas with accuracy below 95% are marked in red. Grey areas represent no data.

For the combined VNIR/SWIR the multi-temporal geometric accuracy is compliant with the requirements. A map of regions with decreased multi-temporal geometric accuracy is presented in

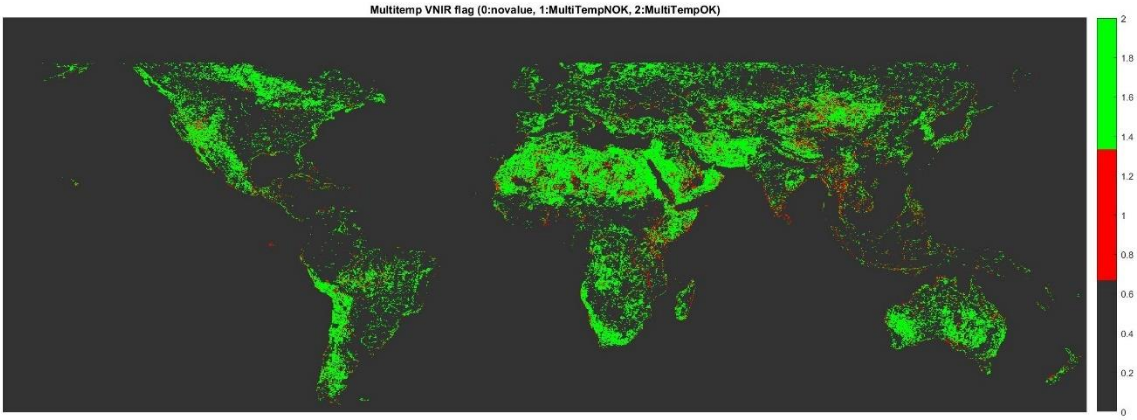

Figure 28.

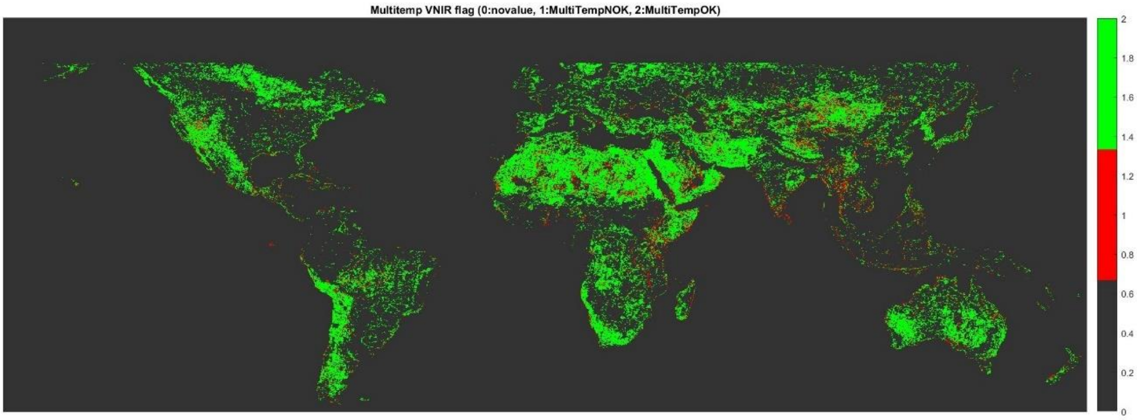

Figure 28: Multi-temporal geometric accuracy for the VNIR/SWIR combined for 16/3/2019 – 15/6/2019. Compliant areas are marked in green; areas with accuracy below 95% are marked in red. Grey areas represent no data.

2.4. Geometric ICP file

On 08.09.2016 a new file with validity date set to 01.09.2016 was created.

ICP filename	Description
PROBAV_ICP_GEOMETRIC#LEFT_20160901_V01 PROBAV_ICP_GEOMETRIC#CENTER_20160901_V01 PROBAV_ICP_GEOMETRIC#RIGHT_20160901_V01	Correction for the gradual degradation observed in the last week of August and first week of September 2016.

3. Reference documents

RD-1	PROBA-V Commissioning Report Annex 1-Radiometric Calibration Results [N77D7-PV02-US-20-CRPT-Annex1-RadiometricCalibartion-v1_3]
RD-2	PROBA-V Commissioning Report Annex 2-Geometric Calibration Results [N77D7-PV02-US-20-CRPT-Annex2-GeometricCalibartion-v1_3]
LIT1	Govaerts Y., Sterckx S. and Adriaensen S. (2013) "Use of simulated reflectances over bright desert target as an absolute calibration reference" Remote Sensing Letters, Vol. 4, Iss. 6, 2013.
LIT2	S. Adriaensen, K. Barker, L. Bourg , M. Bouvet, B. Fougnie, Y. Govaerts, P. Henry, C. Kent, D. Smith, S. Sterckx. "CEOS IVOS Working Group 4: Intercomparison of vicarious calibration methodologies and radiometric comparison methodologies over pseudo-invariant calibration sites A Report to the CEOS/IVOS Working Group", 2012
LIT3	Sterckx S., Adriaensen S., Livens, L., "Rayleigh, Deep Convective Clouds and Cross Sensor Desert vicarious calibration validation for the PROBA-V mission." IEEE Transactions on Geoscience and Remote Sensing. Inter-Calibration of Satellite Instruments Special Issue. Vol.51:3, 1437 – 1452.

Table 18: Reference Documents